A PRECISION MEASUREMENT OF THE WAVELENGTHS OF GAMMA AND X-RADIATION FOLLOWING DECAY OF IRIDIUM 192 AND TUNGSTEN 187, BY MEANS OF THE FOCUSING CRYSTAL DIFFRACTION SPECTROMETER.

Thesis by

David Eugene Muller

In Partial Fulfillment of the Requirements

for the Degree of

Doctor of Philosophy

California Institute of Technology

Pasadena, California

1951

Acknowledgments

The author is indebted to many persons associated with the California Institute of Technology. In particular, he wishes to express his appreciation to Dr. D. A. Lind for his interest and active assistance throughout the early part of the work, and to Mr. D.J. Klein for his aid in carrying out the measurements.

Foremost, however, the author is deeply grateful to Dr. J.W.M. DuMond, who suggested this research topic, and whose inspiring guidance and advice throughout the course of the investigation have been invaluable.

The author also wishes to thank Miss Mary Nakahiro for her patient typing of the manuscript, and Mr. J.R. Brown for the use of a drawing from his thesis.

This work was assisted by the joint program of the Office of Naval Research and the Atomic Energy Commission.

Abstract

Precision determinations of gamma ray and x-ray wavelengths in the spectra following decay of iridium 192 and tungsten 187 are recorded. Measurements of these wavelengths were made with the focusing crystal diffraction spectrometer.

Development of a scintillation counter for use as a gamma ray detector in the spectrometer is described.

The precision of measurements with the spectrometer is analyzed; particular attention being paid to errors resulting from statistical variations in counting rate. Linearity of the instrument is studied by comparing measurements obtained with first, second and third order reflections in the crystal.

Gamma ray energies are combined so as to form decay schemes for iridium 192 and tungsten 187.

TABLE OF CONTENTS

Part	Title	Page
I	GENERAL DESCRIPTION OF APPARATUS	1
	A. Introduction	1
	B. Design of the Spectrometer	2
	C. Geometry of Curved Crystal Spectrometers	5
	D. The Detector	11
	E. Electronics	41
	1. Preamplifiers	44
	2. Coincidence Circuit	45
	3. Main Amplifier	51
	F. Automatic Observer	54
	1. Timer	55
	2. Screw Set Mechanism	55
	3. Additional Parts of the Automatic Observer	56
II	ANALYSIS OF ERRORS IN WAVELENGTH MEASUREMENTS	58
	A. Calibration of the Spectrometer	58
	B. Errors in Wavelength Measurement Produced by Statistical Variations in Counting Rate	64
	C. Causes of Line Breadth	80
III	CENTRAL PROBLEM OF LUMINOSITY	88
	A. Advantages of High Luminosity	88
	B. Intensity Calculations	89
	C. Procurement of Radioactive Materials	96

TABLE OF CONTENTS

Part	Title	Page
IV	DESCRIPTION OF RESULTS	97
	A. Preparation of a Source of Iridium 192 and its Investigation with the Curved Crystal Spectrometer.	97
	B. Decay of Iridium 192	99
	C. Gamma Radiation Following the Decay of Iridium 192	100
	D. Precision of Measurements	114
	E. Study of the Gamma Ray Spectrum of Tungsten 187 .	117

I. GENERAL DESCRIPTION OF APPARATUS

A. Introduction

Crystal diffraction, used so long for precision study of x-ray spectra, has been employed since 1947[1] to impart the same precision to the realm of nuclear gamma rays. Measurements of this sort were made with the focusing crystal spectrometer, which combines high luminosity with the ability to operate at extremely small diffraction angles[2]. This instrument was designed and built by Dr. J. W. M. DuMond with the intention of forming a link between x-ray wavelengths and the range of medium energy gamma rays.

Standard gamma ray energies measured in this way have proved useful in the calibration of beta-ray spectrometers, which in turn permit the study of many gamma ray spectra inaccessible to the crystal spectrometer.

The instrument is principally limited by its requirement of strong gamma ray sources. Even at the present stage of development, which represents a considerable gain over the original sensitivities secured in the earlier 1947 work, not only are sources of at least 10 millicuries of gamma activity required, but also, this activity must be concentrated within the focal volume to a specific activity of 30 millicuries per cm^3. Difficulties due to low intrinsic luminosity become increasingly serious at shorter wavelengths because of decreased reflectivity of the crystal. Dr. D. A. Lind has shown this reflectivity to be proportional to the square of the wavelength[3,4]. To counteract this disadvantage, the geometry of the instrument has been designed to

give the highest attainable luminosity consistent with high precision. Since this design has been discussed at length elsewhere[1,4,5], only enough description will be included here to make the subsequent material understandable.

B. Design of the Spectrometer

A 2 mm thick slab of quartz is cut from a single crystal so that the (310) planes which are used for the diffraction are perpendicular to the faces of the slab*. These faces are then ground optically flat and the slab is bent elastically so as to conform accurately to a part of a cylinder having a 2 meter radius. The (310) planes are maintained parallel to the axis of the cylinder so that if projected they would intersect there. In Fig. 1, this crystal is represented schematically at C. The axis of the cylinder passes perpendicularly through the paper at β . By bending the crystal in this fashion, all the crystal planes are forced to make the same angle θ with rays coming from the gamma ray source at R lying on the focal circle. Selective internal or "Laue" reflection occurs from the entire crystal for a particular wavelength at each angle θ, the wavelength being determined by the Bragg law. Use of the entire crystal in this way produces a gain in luminosity of many times that attained by flat crystal spectrometers.

---

* The (310) planes were chosen because they combine high reflectivity with small grating constant ($d = 1\ A^{\circ}$), giving the instrument high dispersion, and allowing separation of direct and reflected beams even at high energies.

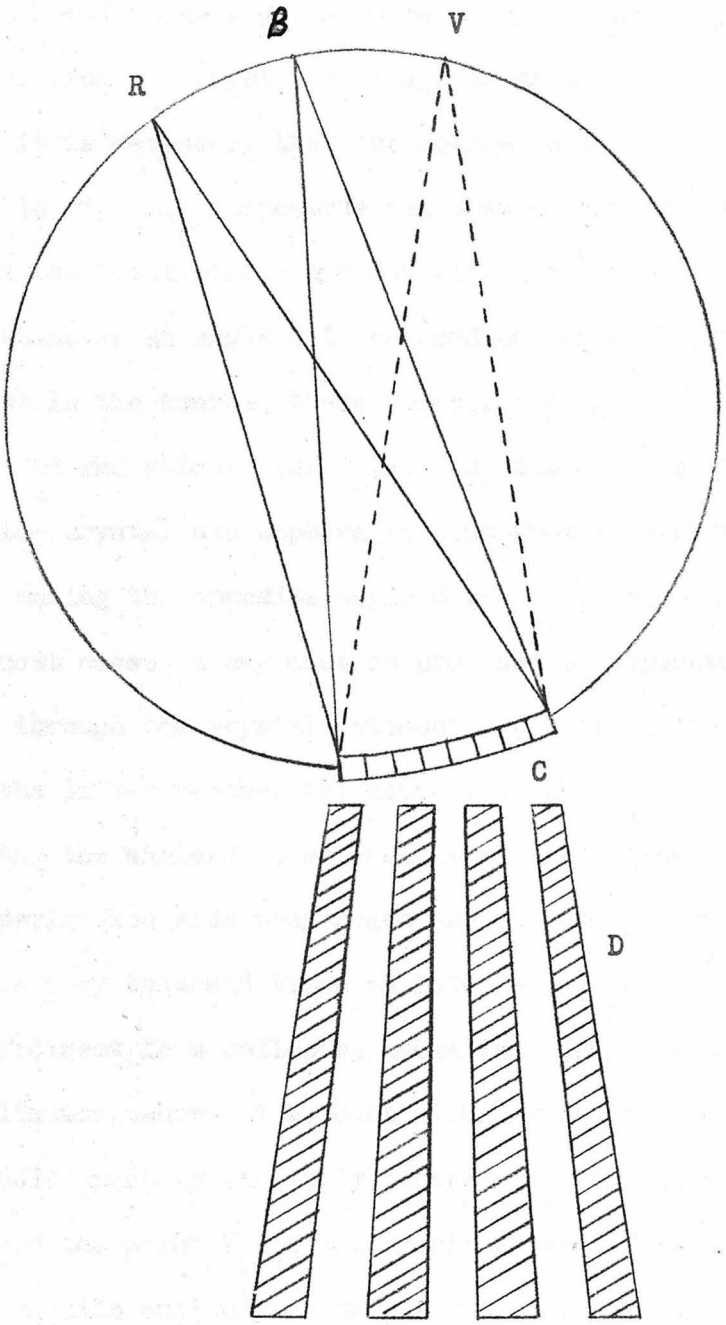

Fig. 1. Illustration of the basic geometry of the gamma ray spectrometer. R represents the source position, C the crystal, B the point of convergence of the crystal planes, V the virtual focus, and D the collimator.

In order for the angle θ to be precisely defined, the source as seen from the crystal must appear as a very narrow line. Furthermore, it is necessary that the source be located on the focal circle shown in Fig. 1. A spectrum can then be explored by moving the source on the focal circle and detecting the intensity of reflected radiation. Whenever an angle θ is reached corresponding to a wavelength present in the source, there appears a sharp increase in selectively reflected radiation. The reflected beam diverges from the convex side of the crystal and appears to come from a point V on the focal circle making the opposite angle θ with the crystal planes.

In most cases, a way must be provided to separate the direct beam passing through the crystal without deflection, from the reflected beam, before the latter reaches the detector. When working with gamma ray wavelengths the angle θ is so small that the two beams would still be mostly superimposed when they reach the detector, were the direct beam (which is many thousand times as intense) not suppressed. This separation of direct from reflected beams is accomplished by what is called a collimator, shown at D, consisting of a number of tapered lead sheets held apart by similarly tapered spacers and arranged to converge toward the point V and thus admit a large fraction of the reflected beam while entirely obstructing the direct beam which is absorbed by the lead sheets. The detector then receives only the reflected beam and possibly a small amount of scattered radiation from the direct beam. It is important to realize that the collimator in no way determines the resolution of the spectrometer, but merely permits operation at the extremely small diffraction angles necessary with

gamma rays. In addition to suppressing the direct beam, the collimator and general geometry of our instrument also avoid a rather annoying difficulty present in the ordinary photographic curved crystal spectrometer as used by Cauchois. In the ordinary type, there appear on the film (placed on the focal circle) lines and oblique bands which are formed by reflections (in different orders) from planes of many Miller indices beside those (310) chosen for use. The geometry and kinematics of the gamma ray spectrometer and the collimator suppress all of these.

A scintillation counter, to be described in detail later, is used as a gamma ray detector because of its high sensitivity. The sensitivity of the detector is important because of the need for the highest obtainable overall luminosity. (This counter is placed directly behind the collimator).

In the actual spectrometer, the collimator and detector remain stationary while the crystal turns and the source maintains a proper relationship to both. The mechanical construction of the instrument is such that all of these motions take place automatically when the precision setting screw is turned. These mechanical features are described in the above references.

C. Geometry of Curved Crystal Spectrometers

Although many different types of focusing crystal spectrometers have been built for various purposes, those true spectrometers using a single curved crystal consist, for the most part, of two types whose designs have been altered little since their original conception. Both the transmission and reflection types were conceived simultaneously

by DuMond and shown to represent two specializations of a single idea[1,6]. Here it will be proved that, subject to rather severe restrictions, these two types are the only designs possible which give an increase in luminosity due to the bending of a crystal. A similar proof was given by DuMond in 1930.

Both designs have two conjugate foci, one of which, in the transmission type instrument is, however, a virtual focus. Two foci are produced by closely confining the crystal lamina to a circle passing through the source (standing at one focus), the crystal and the second focus. Since the Bragg condition requires equal angles of deflection of all the reflected rays, it can easily be seen that this requirement is sufficient to produce the focusing action, provided reflection takes place. In order for reflection to take place, however, the crystal planes must make equal angles with incident and reflected rays and for this reason the crystal planes cannot make a constant angle with the faces of the crystal sheet. In the analysis by DuMond, it has been shown that this requirement forces all the crystal planes, when projected, to intersect at a point on the focal circle midway between the two conjugate foci. Fig. 2 shows the proper orientations of the crystal planes at various points on the focal circle. If the crystal slab lies on the same arc between the foci as the common intersection of the crystal planes, we have an example of the reflection type spectrometer with two real foci. If it lies on the opposite arc, as is true in the gamma ray spectrometer, the reflected radiation has a virtual focus and passes through the crystal. In order to satisfy both the condition upon the crystal planes and the condition upon the faces of the crystal, the crystal must be ground in the shape of a cylinder

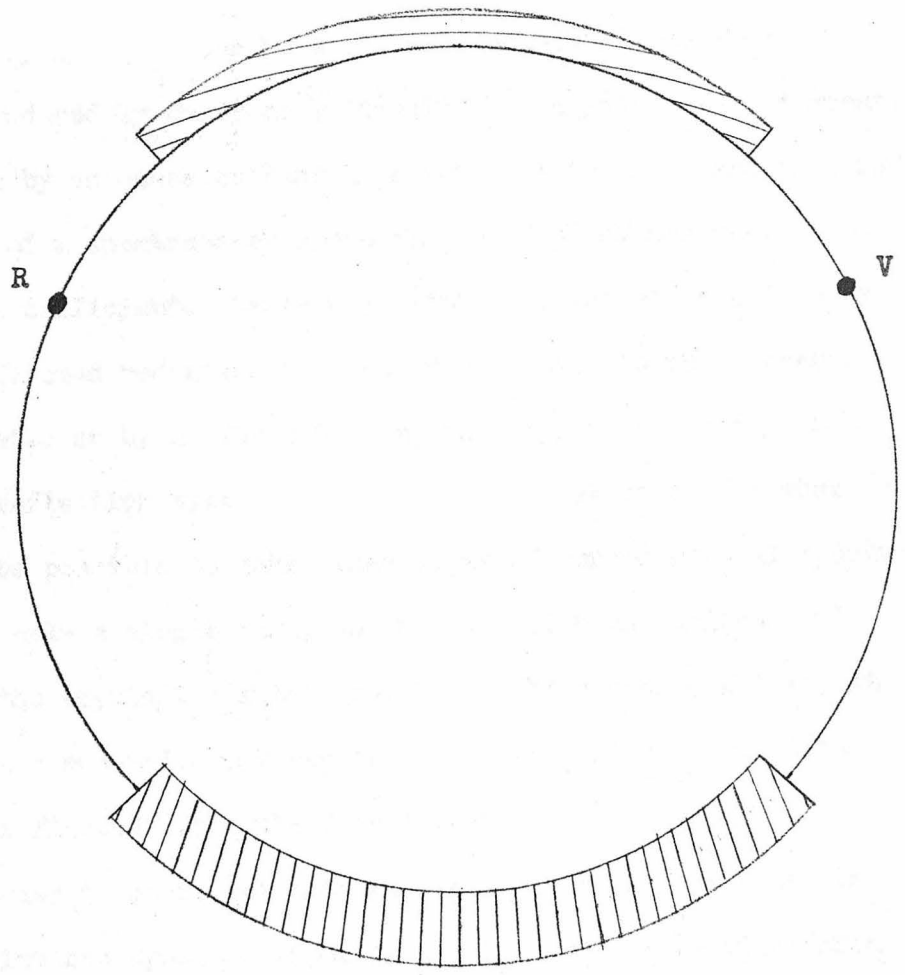

Fig. 2. Diagram showing proper orientation of crystal planes lying at various positions on the focal circle for foci at R and V.

having twice the radius of the focal circle and then mechanically stressed to lie on an arc of the focal circle. This has not been done in the gamma ray spectrometer because, as Cauchois[7] has shown, the aberrations produced by using an initially flat crystal are not great.

It is by no means evident a priori that two foci are required in the design of a spectrometer since for purposes of measurement one focus would be sufficient. Certainly, little advantage is gained by having the reflected radiation diverge from a point in the transmission type spectrometer or by having out-going rays appear to come from a point in the reflection type. We may therefore ask ourselves whether it might not be possible to make other types of curved crystal spectrometers having only a single focus and perhaps with non-cylindrical curvature of the crystal. If this were done the source could lie at the focus, and a non-uniformly tapered collimator might be used to separate the reflected, from the direct beam.

In order to carry out this analysis it is necessary to place certain restrictions upon the types of arrangements to be considered. They are:

1. A single reflection of the beam from the source will occur. This avoids consideration of double crystal spectrometers.

2. No re-bending of the crystal will be required when the wavelength setting of the spectrometer is changed.

3. The two Bragg conditions are assumed to hold:

   (a) The deflection angle 2θ must be constant for any particular wavelength. (It is given by the well known formula $2\theta = 2 \sin^{-1}(n\lambda/2d)$).

(b) The crystal planes must make equal angles with incident and reflected beams.

In addition to these three restrictions, the entire problem will be considered only for the two dimensional case, so that all motion of the source and crystal will be assumed to lie in a single plane. The bending of the crystal will be in the form of a generalized cylinder with its generators perpendicular to the plane of the paper.

Clearly, this is only a very special case of the much more difficult general problem in three dimensions. It is hoped that by its solution insight may be gained into the three dimensional problem. Of the three restrictions which have been listed, the only new one is number 2, which replaces the requirement that the curved crystal have two foci. It is a reasonable condition since the bending of the crystal must be done very accurately and could not easily be performed while the spectrometer is in operation.

Let us regard a typical ray emitted from the source at A in Fig. 3 and reflected from a crystal plane at C. We choose the plane of the paper to be the one containing both the incident and reflected rays. A neighboring crystal plane at C' also reflects a ray from A. Both crystal planes are taken as being perpendicular to the plane of the paper and, because the entire crystal is to be used at once, both of these planes make the same angle θ with their incident rays. Other portions of the source, in order to be used at the same time, must lie very near to A, since no neighboring points make exactly the same angles with both crystal planes.

When a new wavelength corresponding to a new angle θ' is

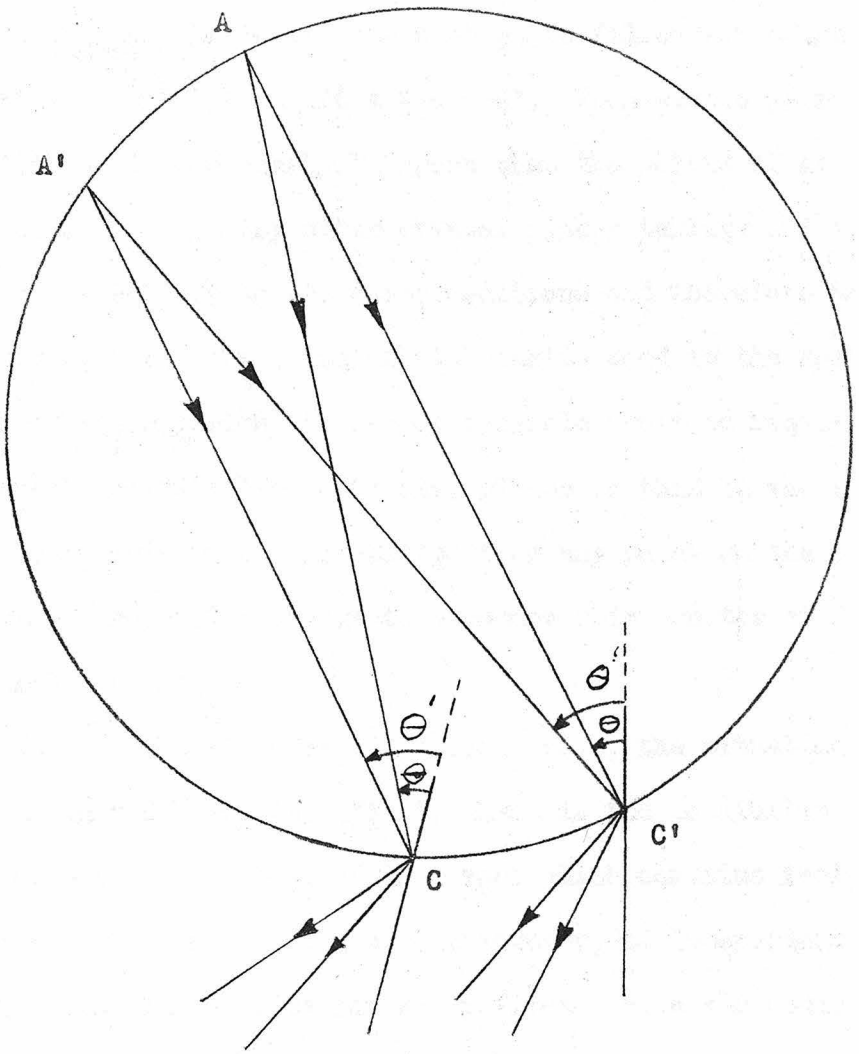

Fig. 3.

investigated, the source point which was at A is moved to a new position A'. The same conditions must be fulfilled for point A' and consequently $\angle A'CA = \angle A'C'A = \theta - \theta'$. From simple geometrical considerations, it can easily be shown that the points A, A', C, C' must lie on a circle. Any other crystal planes taking part in this reflection are subject to the same conditions and therefore must also lie on this circle. Thus, the crystal lamina used in the spectrometer must coincide nearly with the arc of a circle provided requirements 2 and 3 are to be fulfilled. Crystal planes in this lamina must all make the same angle with rays emitted from any point on the circle and consequently they must converge to a common point on the circle, thus completing the proof.

In the general three dimensional case, the situation is more complicated in two respects. First, there is the possibility of focusing into or out of the plane of the paper which contains incident and reflected rays. Such focusing would, however, be independent of focusing in the plane of the incident and reflected rays and could be treated separately. Second, there is the possibility of moving the source out of the plane of the paper. When this is done the geometrical situation becomes much more complicated, but it seems unlikely that any advantage could be achieved in this way.

D. The Detector

After selective reflection from the quartz crystal, the monochromatic gamma ray beam generally has very low intensity in spite of the high activity of the sources used. Therefore, a very sensitive

gamma ray detector is required in the gamma ray spectrometer. The beam, by the time it passes through the collimator and reaches the detector, has a 3" x 3" square crossection. The problem of constructing a sensitive detector, capable of intercepting a large beam, and yet having a low background due to local and cosmic radiation, thus presents itself.

When the first measurements of a gamma ray wavelength were made with the spectrometer, the detector used in the instrument was a geiger counter of an unusual multicellular design[1,2]. This counter was constructed inside a brass tube, 3.25" I.D. closed at one end, which was placed so as to allow the beam of radiation to pass axially down the tube. Covering and sealing the front of this tube was a thin metal window which admitted the beam to the counter. Inside this container were placed coaxially a number of equally spaced thin lead disks which divided the counter into pillbox shaped cells. Anode collecting wires for each cell were made in the shape of crosses and attached to a steel rod which passed down the axis of the counter through $\frac{1}{2}$ inch holes in the centers of the lead discs.

After entering the counter, the gamma ray beam ejected photoelectrons, Compton electrons, and, in the case of high energy radiation, even pair electrons from the lead discs as it passed through them, thus triggering the counter. By using several cells in this fashion the same effect was achieved as if several conventional counters had been placed in the beam, thus increasing the sensitivity many times over that of a single cell counter.

Background due to local radiation was reduced by shielding the

counter in all directions with at least 2½ inches of lead. Counts caused by cosmic radiation were prevented from registering by use of a bank of anticoincidence counters placed around the main counter. These anticoincidence counters were simple cylindrical geiger counters placed so as to be entirely out of the gamma ray beam. Most of the cosmic rays passing through the main counter had to pass through at least one of the anticoincidence counters. Cosmic rays, which consist mostly of ionizing particles, thus would trigger both an anticoincidence counter and the main counter. The electronic circuits were so designed that an anticoincidence count would temporarily block the circuit from the main counter and prevent the count from registering.

In the first gamma ray measurements, a one curie source of gold 198 was used with a four cell counter for the detector. Although quite good contrast was obtained in this particular instance, it was evident that sources of less than 100 millicuries could not be used with such an arrangement. Although many isotopes may be obtained in strength greater than 100 millicuries, the maximum volume available to the source is only 0.3 cm^3 or less, so that at that time sources having a specific activity of less than 300 millicuries per cubic centimeter could not be used. The list of sources available with this specific activity is extremely short and the value of the spectrometer depended very decidely upon the possibility of increasing the luminosity of the instrument. One of the most direct ways to achieve this increase was to improve the detector and this work has been carried on constantly during the time the spectrometer has been in operation. Such an improvement constituted one important phase of the work covered under

this thesis.

The first significant advance in counter design, for use in the spectrometer, came in 1947 when a nine cell counter of the type described above was successfully constructed by D.A. Lind[8]. Design problems connected with this counter were great, since the counting plateaux of the individual cells had to coincide very closely in order to give a sufficiently long overall plateau for the entire counter. This counter was estimated to have an efficiency of 25% at 0.5 Mev and 10% at 1 Mev, where efficiency represents the fraction of those photons passing through the counter which are counted. Because of its special design, however, it was plagued with many of the usual counter troubles to an exaggerated degree. Its lifetime was short, never more than 10^7 counts, and therefore it required frequent refilling; often at the most awkward times as for example, while a short lived source was being investigated.

Another difficulty with this counter was the presence of "bursts" in the counting, which consisted of a large number of spurious counts occurring in rapid succession. Although it is doubtful that these bursts were frequent enough to cause any really great errors in the count totals, they caused considerable concern.

In the fall of 1949, work was started by Lind and Brown on several multicellular counters of new design. These counters are described in detail in Brown's thesis. They were enclosed in 10 inch long cases of 3" x 3" square crossection so as to intercept the square beam of gamma rays which emerges from the collimator. These cases, which were copper plated on the inside, were designed to contain up to thirty

equally spaced thin square plates placed so as to separate the counter into cells. Different materials such as lead, tantalum, copper plated tantalum, silver, bismuth, and copper were used for the plates in different counters depending on the energy of gamma ray to be detected. Four symmetrically spaced anode wires were run the length of each counter through 3/8 inch holes in the plates. A large number of plates were thus available for ejection of electrons by the gamma rays and the overall efficiency of the counter was greatly enhanced. Certain difficulties connected with the successful construction of these complex counters, however, proved to be nearly insurmountable. Of the many counters of this type which were assembled, taken apart, and reassembled many times over, only one counter operated properly for more than a few days. This counter which contained twenty-five 5 mil copper plates was, for no apparent reason, unique since its operation was trouble-free, for many months, and for over 10^7 counts. It was used up to the time of installation of the present detector to study the gamma rays from tantalum 182, rhenium 188, tungsten 187, and radon. The long life of this counter may have been due to the use of a special type of quench circuit which reduced the counter voltage by 250 volts in less than 0.3 microseconds after the beginning of the counter discharge, thus quenching it before a significant amount of the quench gas could be used up.

In spite of having greatly increased the luminosity of the spectrometer, the requirement of strong concentrated sources though much ameliorated remained still the greatest problem connected with the instrument. This fact became very apparent when the spectrometer failed to detect several of the very interesting soft lines of tantalum 182,

which were just the ones needed to check certain proposed decay schemes. Investigation was therefore started in the spring of 1950 into the possibility of using a scintillation counter as the detector in the spectrometer.

A sodium iodide crystal containing a small amount of thallium impurity commonly described as NaI (Tl) was chosen as the phosphor for the scintillation counter. This choice was based upon a number of considerations. In the first place, the material used should have a high absorption coefficient for gamma radiation so as to make possible the counting of a large fraction of the photons in the beam. Secondly, the material should have a large scintillation efficiency; that is to say, a large fraction of the energy of the gamma photon should be converted into light photons by the phosphor. This property is important, since many of the gamma ray energies measured by the spectrometer are quite low, and a large scintillation efficiency is necessary, if the light signal is to register above the noise background. Finally, the material should be available in large enough samples so that the entire 3" x 3" beam of radiation may be intercepted by the detecting material. It is not important that the phosphor have a fast resolution time since the counting rates with the gamma ray spectrometer are never high.

Scintillations from NaI (Tl) were first noticed and investigated by Hofstadter in 1948[9]. He reported obtaining much larger pulses of light from sodium iodide than from any of the organic phosphors known at that time. Organic phosphors such as anthracene, stilbene, and p-terphenyl, not only gave smaller light pulses but had lower gamma ray absorption coefficients than sodium iodide. (The short decay time of

these phosphors was of no advantage to this type of detector). Although potassium iodide, which has also been investigated as a phosphor by Hofstadter, has a slightly higher gamma absorption coefficient than sodium iodide, its pulses are quite significantly lower and for this reason it must be considered decidedly inferior.

A rectangular 3" x 3" x 1" NaI (Tl) crystal was purchased from the Harshaw Chemical Company, where crystals as large as this one are grown artificially. Phosphors of this size are not common and it probably represented the largest crystal ever used for scintillation work. Quite apart from other objections to the use of organic crystal phosphors, the size of crystal needed by the detector would probably have excluded their use. A p-terphenyl solution in xylene could have been obtained in suitable quantity, but it would have had the disadvantages described above.

Permanent mounting of the crystal presented many problems. The surfaces of the crystal are hygroscopic and if the crystal is left exposed to the air for a short time it picks up a layer of moisture on its surface. Other investigators have found that even if such a crystal is mounted in a plastic box the crystal surface manages to pick up moisture which may possibly have been absorbed in the plastic. Since a slight amount of moisture makes the surface of the crystal quite cloudy, it is necessary to mount the crystal in a glass box so as to avoid impairing the reflecting and transmitting properties of the crystal surface. Plates of glass used for the sides of this box were grooved with a diamond saw so as to fit together and then cemented with insalute cement, providing a water-tight mounting for the crystal. Before being

placed in this box, the crystal was rubbed with progressively finer sandpaper to smooth its surface irregularities. The crystal was polished with cotton under xylene, to remove surface cloudiness. In order to improve the polishing action of the xylene and to bring the crystal to the temperature of the mounting fluid which had been placed in the glass box, the xylene containing the crystal was heated slightly. This mounting fluid was a type of semi-fluid resin called chlorinated biphenyl which is viscous at room temperatures but which becomes fluid when its temperature is raised. A suitable medium is thus provided to match the optical index of the crystal and to exclude air from the glass box. Unfortunately, when the crystal was removed from the hot xylene in order to place it in the glass box, the cooling due to the evaporation of the xylene from the crystal caused two large cracks to appear diagonally across the crystal face. On previous occasions, this same procedure had been rehearsed successfully using smaller crystals which were naturally less susceptible to thermal shock, but in this case the crystal was too large to permit the use of this method. In spite of the cracking of the crystal, it was placed in the glass box and the cover was cemented in place with Duco cement after all air had been excluded from the region between the crystal and the walls of the box. In the photograph in Fig. 4, the potted crystal may be seen with its main diagonal crack.

In the future, another similar crystal will be prepared using mineral oil instead of chlorinated biphenyl for the mounting medium to avoid the necessity of heating the crystal. Mineral oil is more transparent to the violet and ultraviolet light given off by the crystal as

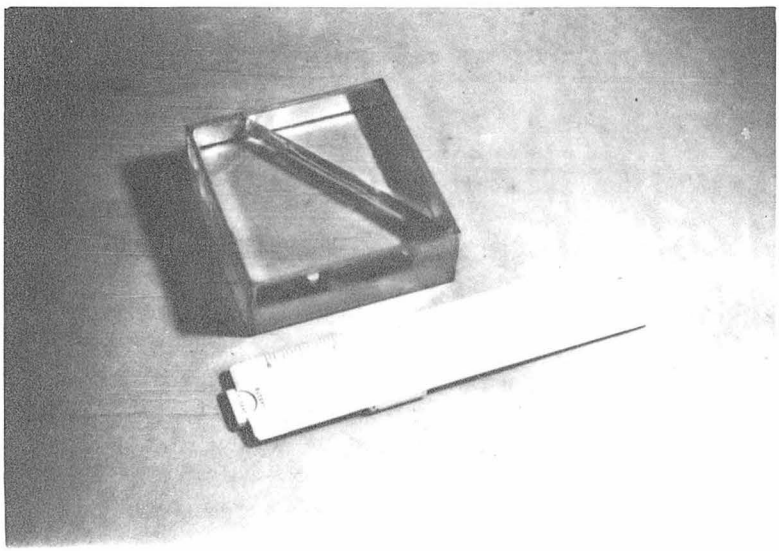

Fig. 4. A photograph of the sodium iodide crystal enclosed in its glass container.

it scintillates and should therefore prove superior. Polishing may be accomplished quite simply by dipping the smoothed crystal in acetone to dissolve a small layer of its surface before placing it in mineral oil. Surfaces of good optical quality have already been produced on smaller crystals in this fashion.

Scintillations of light produced by the crystal are detected by use of two photomultiplier tubes which look through two opposite 3" x 1" faces of the crystal. Individual flashes of light produce electrical pulses in the phototubes, which are amplified in the tubes themselves and in the following electronic circuits. Pulses within a certain height range are then counted in the same way as are the pulses from geiger counters. Two phototubes are operated in coincidence so as to prevent counts from registering, unless they are produced by scintillations observed simultaneously by both phototubes. In this way electrical noise, always present in photomultipliers, is prevented from registering as genuine counting, since noise pulses produced by the two phototubes will not generally coincide in time.

Fig. 5 shows how the ends of the phototubes are pressed against a pair of plexiglass light cones which are used to transmit the light from the crystal to the photosensitive cathodes of the phototubes. These photosensitive cathodes have been deposited on to the inside glass surfaces of the ends of the tube envelopes. Contact surfaces between phototubes and light cones, and between light cones and crystal housing are sealed with a layer of transparent vacuum grease so as to minimize reflections. Light cones used in this arrangement are 1.25" long and are machined so as to fit the phototube at one

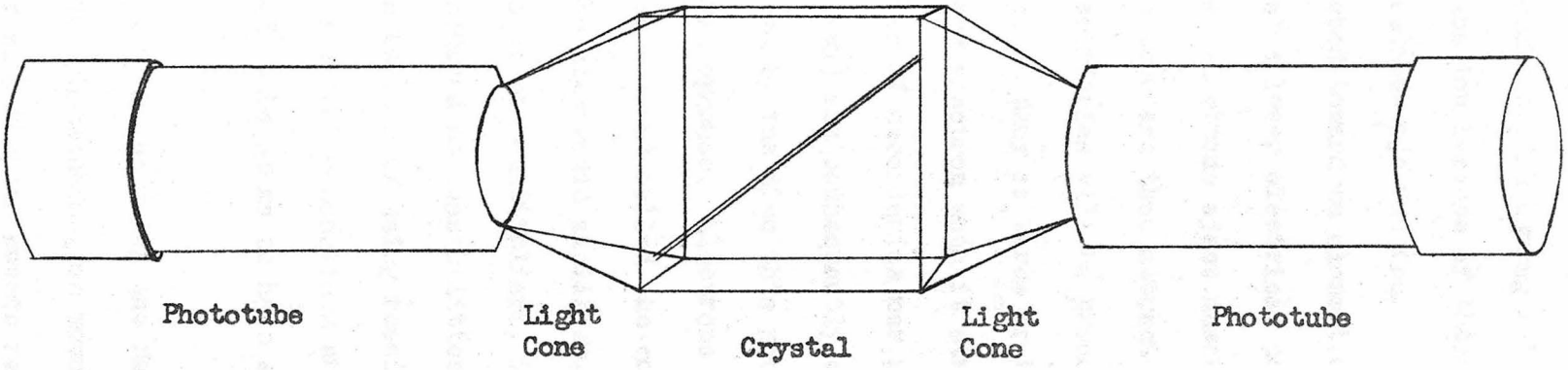

Fig. 5. Drawing of crystal, showing positions of phototubes and light cones in scintillation counter arrangement.

end, and a 3" x 1" face of the crystal housing at the other.

R.C.A. 5819 photomultipliers having a 1.5" circular cathode were chosen for this application because of their high sensitivity and convenient shape. Electrons ejected from the photocathode by the action of light are attracted toward an element of the tube called the first dynode, which lies at a lower electrical potential. Upon striking the first dynode, these electrons eject numerous secondary electrons from its surface, which in turn are then attracted toward the second dynode where still more secondaries will be produced, and so on throughout eleven dynodes. As many as three or four secondaries may be produced for each primary electron when it strikes a dynode, (although the average number of secondaries per primary electron depends on the inter-dynode potential) and consequently current gains of the order of 10^6 may be achieved by the time this process has been continued throughout all eleven dynodes. Electrons from the last dynode are finally picked up by an element called the collector, from which the signal is taken for the electronic amplifier.

Two similar types of photomultipliers, the R.C.A. 5819 and the E.M.I. 5311, were considered as possibilities for use in the detector. The R.C.A. tube was chosen because of being readily obtainable and because of its convenient electrical connections and in spite of the fact that the British made E.M.I. tube seems to have somewhat superior electrical characteristics.

The detecting apparatus including the NaI (Tl) crystal, the two light cones, and the two phototubes, was mounted in a light-tight container. This container with the two covers removed, is shown in

Fig. 6. Later the crystal and light cones were covered with shiny aluminum foil to reflect any light which might escape from the surfaces of the glass box, and also to avoid electrical discharges over the surfaces which were found to occur when voltage was applied to the R.C.A. 5819 tubes.

A 3" x 3" square hole was milled in the front cover of this container. This hole was covered with aluminum foil to exclude outside light but to serve as a window for soft gamma radiation.

Counting rates with the gamma ray spectrometer are low and as a result background must be reduced to a correspondingly low level in order not to obscure the signal. Background is due to a number of causes, it comes from local radiation in the room, radiation scattered from the sides of the collimator, and from cosmic radiation. Protection from the local radiation is afforded by 4" of lead surrounding the detector on all sides. Scintillations produced by cosmic rays are generally much brighter than those from ordinary gamma rays because of the high energies associated with the cosmic rays and for this reason, they produce larger electrical pulses. This property allows cosmic rays to be discriminated against electronically in the present scintillation detector system instead of being cut out with anticoincidence counters as was the case in the earlier G.M. counter systems.

Noise originating in the phototubes consists of discrete pulses very similar to those produced by scintillations. They vary considerably in height, and pulses of lower height tend to be considerably more numerous. A noise pulse is produced when a stray electron is evaporated from the cathode or one of the early dynodes. The amplifying

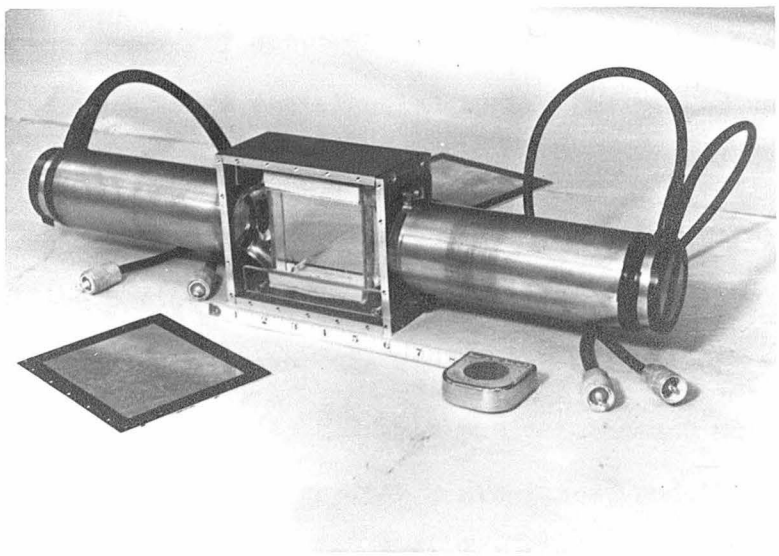

Fig. 6. The assembled scintillation counter with front and back covers removed, exposing the crystal.

action of the dynodes then produces a pulse of current at the collimator. (Fig. 7 shows the relative dependence of noise pulse height and signal pulse height on phototube voltage). It is evident that the signal to noise ratio is reasonably independent of voltage until a critical voltage is reached. Above this voltage, which varies widely from tube to tube, the noise increases very rapidly and the tube may not be used effectively.

Although noise pulses are generally small, a few of them are of height comparable to signal pulses. Due to the low counting rates used with the gamma ray spectrometer, these few large noise pulses would represent a large contribution to the background were they not eliminated in some way.

Noise in phototubes may be combated in two ways: One method is to cool the phototube to dry ice temperatures thereby suppressing the noise producing process, the other, the coincidence method described earlier. It was decided that the coincidence method should be tried first because of its greater convenience, and then if necessary, a cooling apparatus could be installed later. Entirely formless and random noise would have been difficult to eliminate by coincidence techniques. Phototube noise, however, consists of discrete pulses, the time between pulses being much longer than the individual pulses. Simultaneous occurence of such pulses in the two phototubes is so infrequent that for practical purposes it never happens. For this reason, the coincidence method was quite successful and it was never necessary to resort to cooling.

Before putting the scintillation counter into service as a

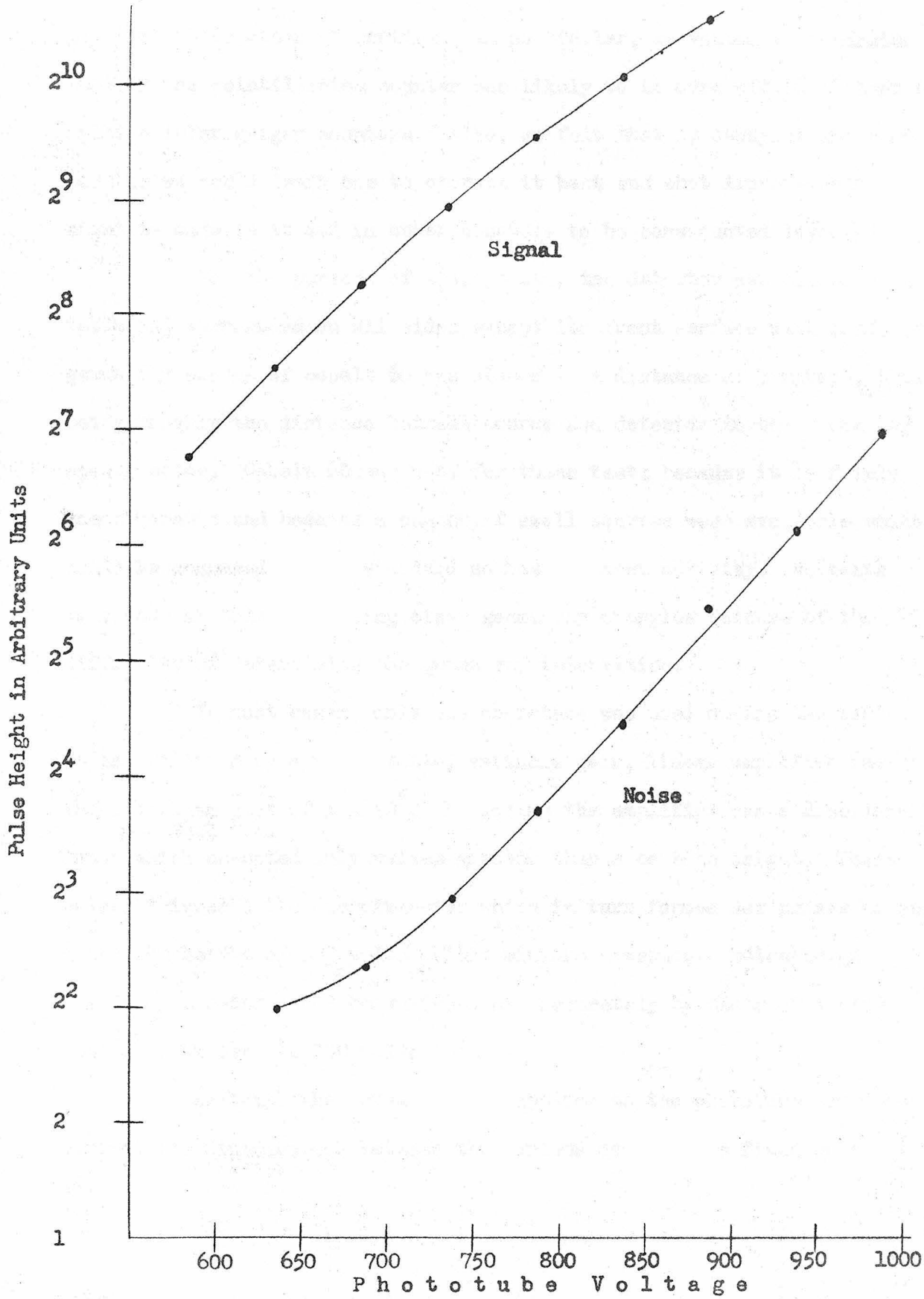

Fig. 7. In the above graphs, 10,000 pulses per minute are larger than the indicated pulse height for a given phototube voltage.

detector in the gamma ray spectrometer, numerous tests were made of its efficiency and other properties. In particular, we wanted to determine whether the scintillation counter was likely to be more efficient than the multicellular geiger counters. Also, we felt that by studying its properties we could learn how to operate it best and what improvements might be made in it and in other counters to be constructed later.

For the purpose of these tests, the detector was placed on a table and surrounded on all sides except its front surface with lead. A gamma ray source of cobalt 60 was placed at a distance of 3 meters, this being roughly the distance between source and detector in the gamma ray spectrometer. Cobalt 60 was used for these tests because it is fairly monochromatic and because a number of small sources were available which could be compared with a standard source of known activity. No tests were made at this time using other gamma ray energies because of the difficulty of determining the gamma ray intensities.

In most cases, only one phototube was used during the tests. It was followed by a very stable, variable gain, linear amplifier having a maximum gain of 3×10^5. Following the amplifier was a discriminator which accepted only pulses greater than a certain height. These pulses triggered the discriminator which in turn formed new pulses having a uniform height of 100 volts. This minimum acceptable pulse height of the discriminator could be varied quite accurately by means of a bias control from zero to 100 volts.

Although the total voltage applied to the phototube could be varied, its distribution between the various dynodes was fixed by a

set of resistors placed in series with each other across the power supply. For these tests, the voltages from cathode to first dynode, to second dynode etc., were held in the ratio 5:3:1:1:1 ---. This ratio was later changed to 2:1:1: --- to allow the phototube to be operated at a higher total voltage. Little change in the other tube characteristics seemed to result from this.

Fig. 8 shows plots of counting rate vs discriminator bias. The ordinate therefore represents the number of pulses obtained which were above a certain minimum height while the abscissa represents this minimum height. Naturally, such a curve is a monotonic decreasing one. It shows the way in which the efficiency of the counter is reduced when the discriminator bias is increased. Such a plot is called an integral pulse height distribution curve or simply an integral curve. By lowering the discriminator bias, one may obtain a more efficient counter; but at the same time this advantage is offset by an increase in the background counting rate. An analysis giving the optimum discriminator setting is described in the section on precision, page 76. This setting is generally in the low bias and high efficiency region.

Absolute efficiency may be defined as the fraction of gamma ray photons entering the 3" x 3" window of the detector, which are counted. To determine the absolute efficiency of the detector, a standard source of cobalt 60, having a known strength of 11.65 Rutherfords, was obtained. A line representing 50% efficiency is shown on the integral pulse height diagram in Fig. 8. A similar line represents the efficiency of the multicellular geiger counter in use prior to installation of the scintillation counter. Discriminator bias settings

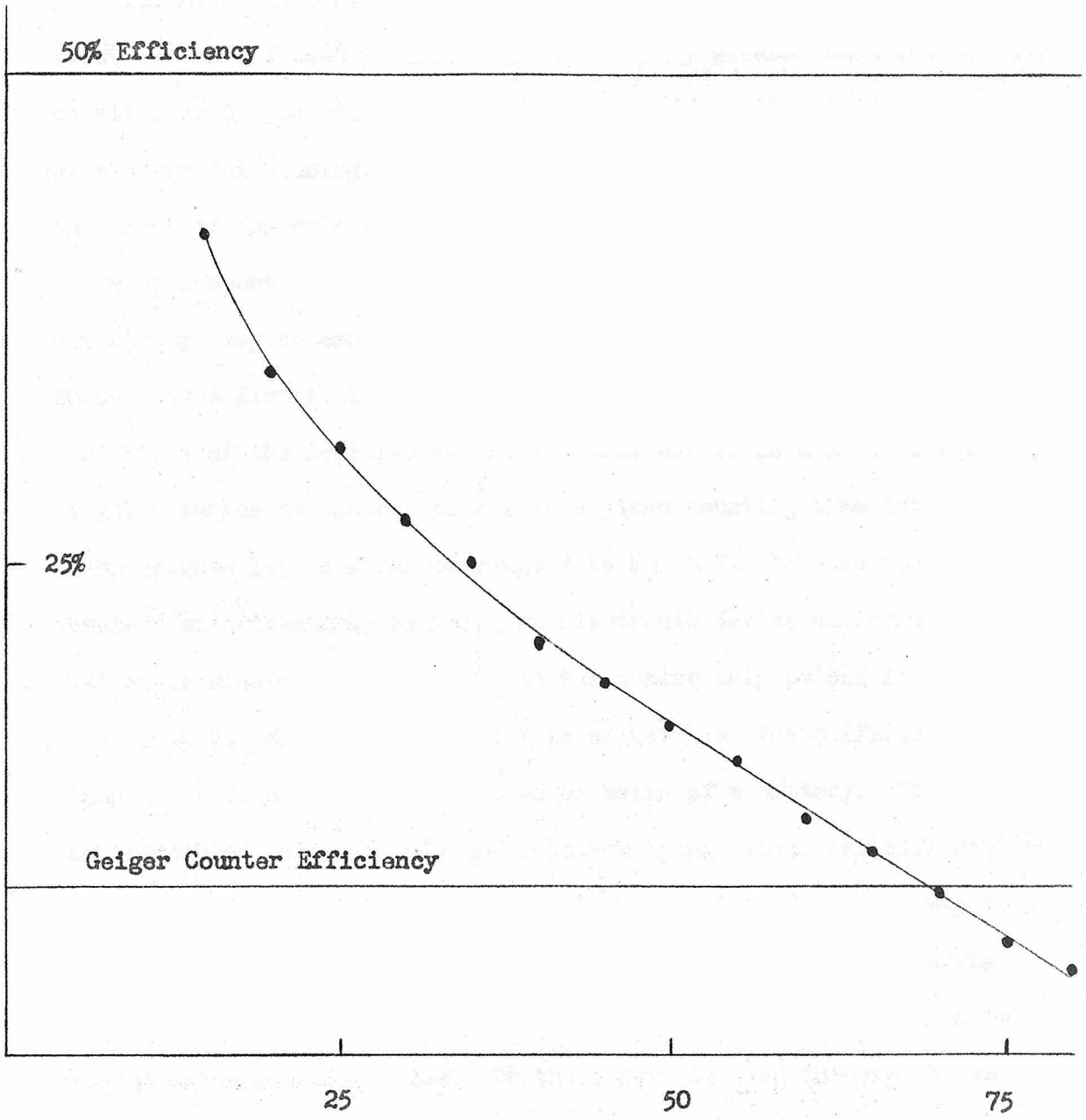

Fig. 8. An integral curve showing the variation of efficiency with discriminator setting for 1.2 Mev. radiation. Phototube voltage was maintained at 800 volts.

giving 40% efficiency may conceivably be used, corresponding to about 5 times the efficiency of the geiger counter. Since the absorption coefficient of the crystal for 1.2 Mev radiation is 0.5 $in.^{-1}$, about 40% of the beam is absorbed. Efficiency greater than 40% could result from the counting of quanta scattered from the sides and back of the crystal housing. It would appear from these considerations that most of the pulses present are counted.

Properties of the scintillation counter, other than its efficiency, may be conveniently studied by constructing a differential pulse height distribution curve. Such a curve, which is roughly the derivative of the negative of the integral curve, is a plot of the height V versus the number pulses in a given counting time interval whose heights lie in a narrow range V to $V + \Delta V$. This curve may be obtained experimentally by using an electronic device called a differential discriminator, which passes to the scalar only pulses in the range V to $V + \Delta V$. While the voltage V is adjustable, the differential window ΔV is held precisely fixed by means of a battery. Therefore, one is enabled to count only those pulses lying within the differential window ΔV. Clearly a differential curve obtained in this way is much more precise than one obtained by mechanically differentiating an integral curve, since this would involve taking small differences between large counting rates. On the other hand, an integral curve of good accuracy may be obtained by integrating a differential curve.

Differential curves taken with small NaI (Tl) crystals, have been used by Hofstadter and others[10,11,12] to measure gamma ray energies. These measurements are possible because the brightness of

the scintillations in NaI (Tl) is very closely proportional to the amount of energy released by the gamma rays in the crystal. Differential pulse height distributions can thus be interpreted as energy spectra, providing the light detecting apparatus is linear.

Gamma ray energy release in the crystal may result from either photoelectric absorption, Compton scattering, or pair production. In each case the energy release, and thus the corresponding pulse height, will be different.

If mono-energetic gamma rays are used, the pulses resulting from photoelectric absorption will be of uniform height corresponding to the total energy of the incident gamma. Although some of the energy of the absorbed quantum gives kinetic energy to the ejected electron, and some imparts work of ionization, all of this energy will eventually be dissipated in the crystal, since the resultant x-ray or Auger electron will not generally be able to escape from the crystal. Compton scattering, however, produces a continuum of pulse heights, provided the degraded radiation escapes from the crystal.

When pair production is possible, the pulse height represents the combined kinetic energy of the positron and electron. These pulses will therefore have a height corresponding to the energy of the incident photon minus the energy required for the creation of an electron-positron pair. An idealized differential pulse height distribution for a single gamma energy would therefore look something like the curve in Fig. 9, with a peak at the high end corresponding to photo-electric absorption, and a diminishing continuum of pulse heights leading away from this peak caused by Compton scattering. A second

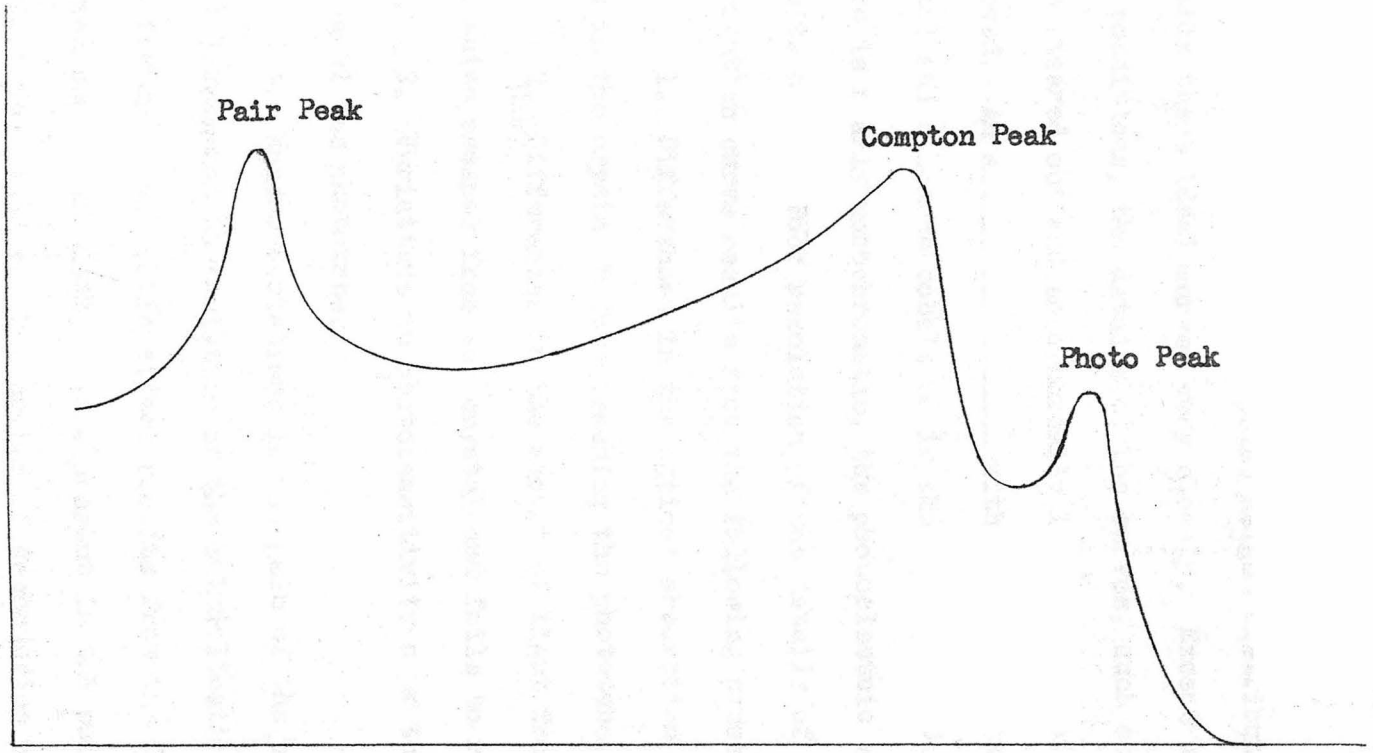

Fig. 9. Idealized differential spectrum of single high energy gamma line showing peaks due to photoelectric absorption, Compton scattering, and pair production. This diagram is taken from ref. 12.

peak due to pair production may be present if the energy of the gamma ray is sufficiently high.

Actual differential pulse height distributions often do not resemble these ideal curves very closely. Except under especially good conditions, the details of the curves, such as the peaks, tend to be smeared out and an abnormally large number of small pulses are observed. An actual curve taken with the 3" x 3" x 1" NaI (Tl) crystal and a source cobalt 60 is shown in Fig. 10. Although this source is nearly monochromatic, the photoelectric and Compton peak is quite broad. Poor resolution of the details of the pulse height distribution curve results from the following causes:

1. Differences in the optical absorption of the scintillations in the crystal before reaching the phototube.

2. Differences in the amount of light from various scintillations which escapes from the crystal and fails to reach the phototube.

3. Variations in photosensitivity over the surface of the cathode of the phototube.

4. Random variations in the gain of the phototube at low signal levels due to variation of the multiplication factor on the first few dynodes. (This effect results from the fact that a small integral number of electrons are present in the pulse of current to the first few dynodes. The number of secondaries produced by the individual electrons varies in a statistical fashion and hence the total multiplication factor also varies somewhat).

5. Apparent variations in pulse height caused by phototube noise or possible noise or hum in the following amplifier.

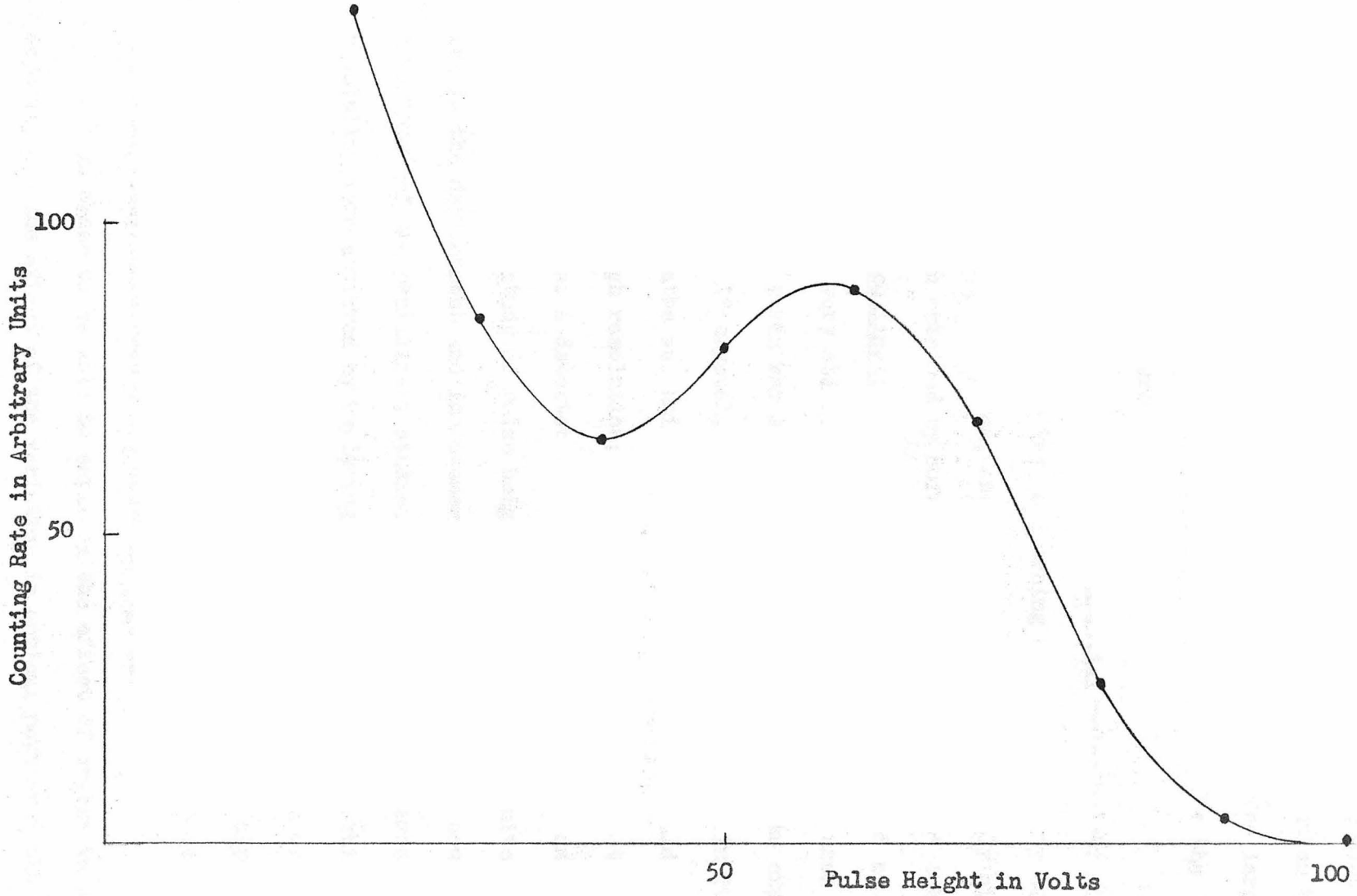

Fig. 10. Differential pulse height distribution obtained using cobalt 60 gamma radiation.

Other factors such as escape of x-rays and ionizing electrons from the surface of the crystal could also damage the resolution but such effects are believed to be of secondary importance. The large number of small pulses observed in Fig. 10 is believed to be the result of radiation scattered from the surroundings.

Resolution of the details of differential pulse height distribution curves are thus the key to learning about the quality of the crystal, the optical system, and the phototubes. Extremely high resolution has been obtained by Hofstadter and others using $\frac{1}{2}$" cubic crystals and well collimated gamma rays[12]. Such scintillation counters used with very stable electronic circuits have been used as high luminosity gamma ray spectrometers. It is too much to expect that the 3" x 3" x 1" crystal, having considerable variation in its internal optical paths and using uncollimated radiation, should be capable of this high resolution; nor is this necessary for it to serve its purpose as a detector for the curved crystal spectrometer. Nevertheless, the study of pulse height curves has proved quite helpful in the development and improvement of the scintillation counter. After most of the preliminary studies had been made, improvements in resolution were achieved by replacing one of the phototubes which seemed to have poor characteristics, and upon the suggestion of Dr. Hofstadter, by surrounding the crystal and light cones with aluminum foil to enhance light reflection. Differential curves taken before and after these improvements are shown in Fig. 11.

In order to be able to estimate the effect of cracks in the crystal, and the effect of the variation in optical path over the face

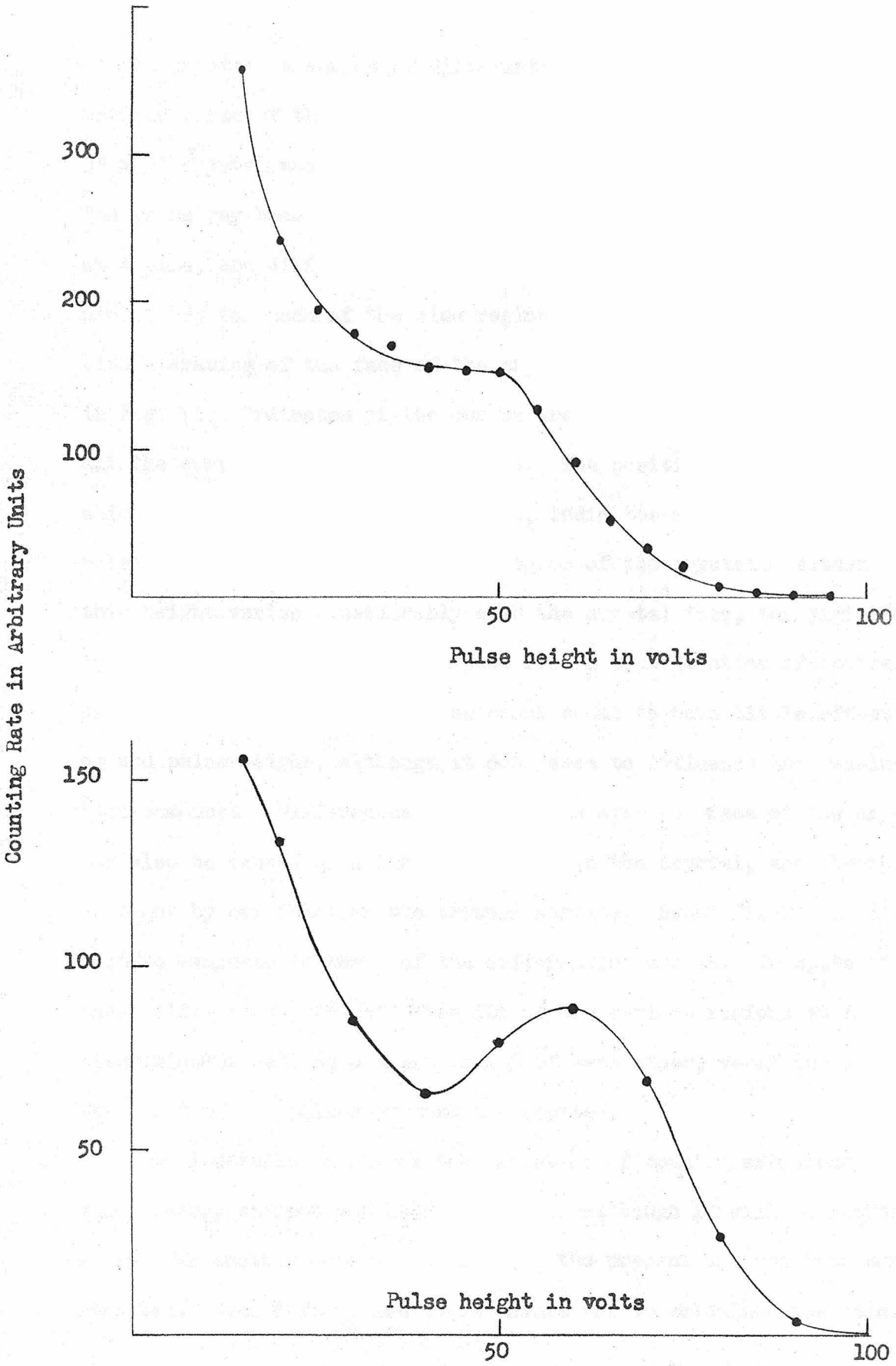

Fig. 11. Differential pulse height distributions from cobalt 60 radiation taken before (above) and after (below) improvements were made on the scintillation counter.

of the crystal, a series of differential curves were plotted for various parts of the crystal. For convenience, the face of the 3" x 3" crystal was marked off into nine 1" x 1" square regions. The gamma ray beam was masked so as to hit only one of these regions at a time, and differential curves were taken for each of the two phototubes for each of the nine regions. These curves together with a drawing of the face of the crystal showing the crack, appear in Fig. 12. Ordinates of the curves are normalized so as to require all the curves to have the same area. The position of the photopeak, which in some cases is merely a bump, indicates a characteristic pulse height obtainable from each region of the crystal. Although this height varies considerably over the crystal face, the variation is not as great as one might expect from a consideration of optical path alone. The presence of the crack seems to have little effect on the pulse height, although it does seem to influence the resolution somewhat. Differences in the curves over the face of the crystal may also be caused by slight cloudiness in the crystal, and absorption of light by particles on the crystal surface. Such effects are difficult to evaluate in terms of the differential curves. In spite of these differences, the efficiencies of the various regions at low discriminator setting are within 20% of each other, verifying again that most of the pulses present are counted.

A detailed study of the variation of counter efficiency with gamma energy has not yet been attempted, although it will be started as soon as another detector similar to the present one has been constructed. Such information would enable one to calculate the relative

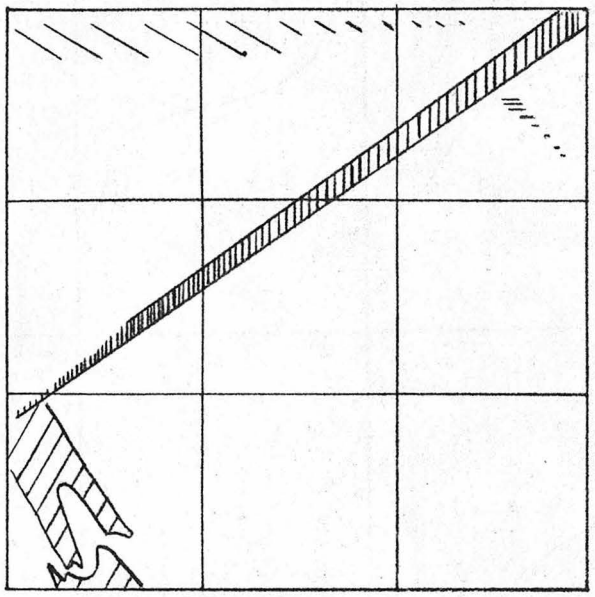

Fig. 12(a). Drawing of the sodium iodide crystal face showing cracks and arbitrary division into nine one inch square regions. Locations of phototubes are indicated on the sides. This drawing allows interpretation of the differential curves of Figs. 12(b) and (c).

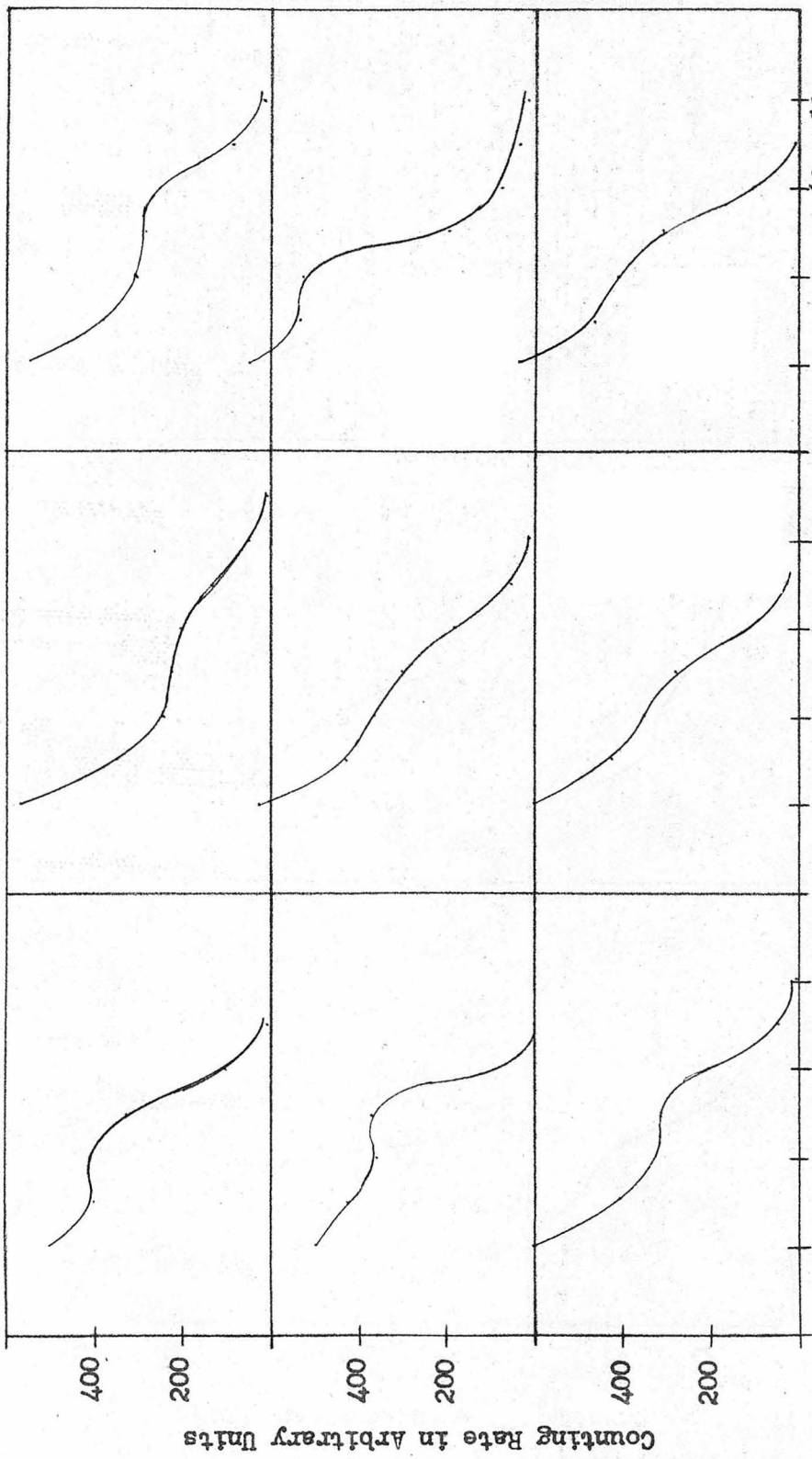

Fig. 12(b). Differential curves of the nine regions of the sodium iodide crystal, using cobalt 60 radiation. These curves were taken using only phototube 1 on the left.

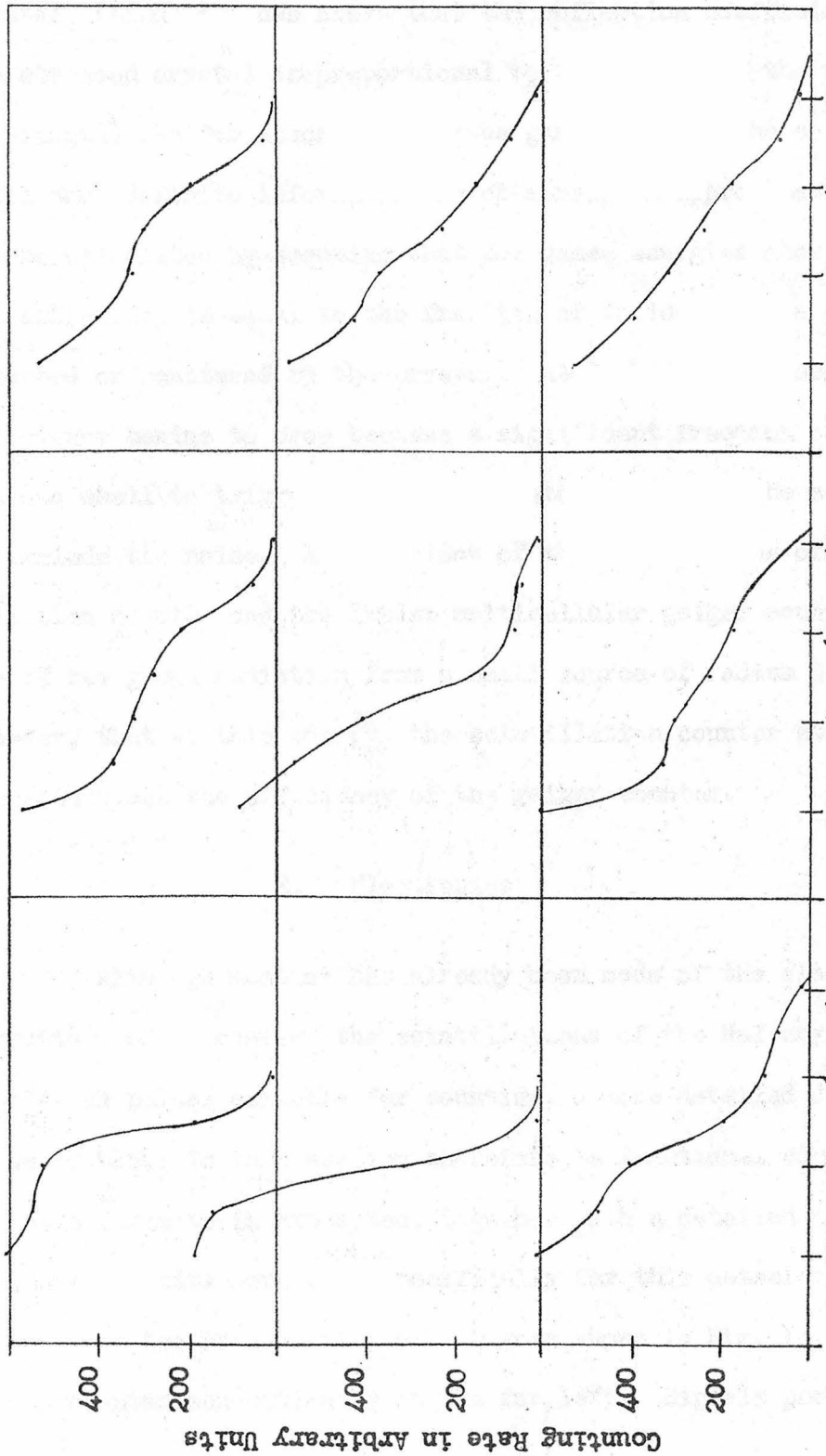

Fig. 12(c). Differential curves of the nine regions of the sodium iodide crystal, using cobalt 60 radiation. These curves were taken using only phototube 2 on the right.

intensities of gamma ray lines observed with the spectrometer. Corrections would have to be made for reflectivity of the curved crystal, (Lind[3,4] has shown that the reflection coefficient of the stressed crystal is proportional to the square of the reflected wavelength) and for absorption of the gamma rays by the source. Until more definite information is obtained, an approximate efficiency may be calculated by assuming that for gamma energies above 50 Kev the efficiency is equal to the fraction of incident gamma rays absorbed or scattered by the crystal. At lower gamma energies the efficiency begins to drop because a significant fraction of the pulses are too small to trigger the discriminator which must be set so as to exclude the noise. A comparison of the efficiencies of the scintillation counter and the latest multicellular geiger counter, using the 47 kev gamma radiation from a small source of radium D, revealed however, that at this energy, the scintillation counter still had thirteen times the efficiency of the geiger counter.

E. Electronics

Although mention has already been made of the electronic circuits used to convert the scintillations of the NaI crystal into electrical pulses suitable for counting, a more detailed description is desirable. In this section therefore, a functional correlation of these circuits is attempted, together with a detailed description of those circuits developed specifically for this detector.

In the functional block diagram shown in Fig. 13, the detector is represented schematically at the far left. Signals produced by the

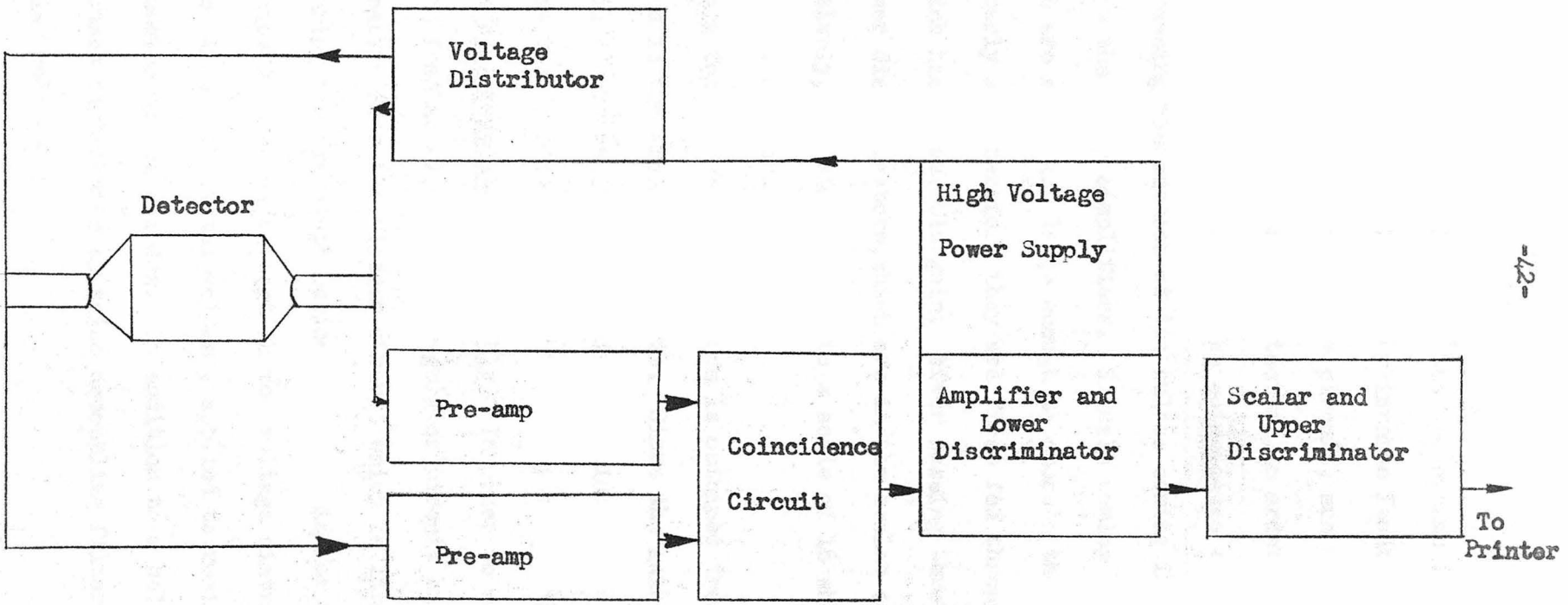

Fig. 13. Functional block diagram of detecting apparatus.

two phototubes are shown passing into the two preamplifiers, each of which has a gain of 3,000 stabilized by inverse feedback. Both preamplifiers, as well as the coincidence circuit, are placed directly on top of the lead housing for the detector, in order to shorten the signal cables as much as possible. The coincidence circuit has the property of passing the smaller of two pulses coming into it simultaneously from the two preamplifiers. Signals coming from the coincidence circuit are still not large enough to operate the discriminator circuits properly and therefore they are first fed through the main amplifier which has adjustable gain. After passing through the upper and lower discriminators, which are in the scalar and amplifier units respectively, the signals go into a scale of 16 which drives a register in the printer.

Voltage for the photomultipliers is obtained from a power supply located in the amplifier chassis. Since the gain of the photomultipliers is a very rapidly increasing function of the total voltage applied across the dynodes, it is of utmost importance that this voltage be as well regulated as possible. In order to achieve this stability, the feedback loop in the regulator circuit has carefully been kept separate from the bleeder circuit which is likely to change resistance during the "warm up" period. Equal gain for the photomultipliers is achieved by an adjustment in the voltage distributor, which allows one to balance the total voltages applied to resistance voltage dividers connected to the dynodes. In addition to a balancing adjustment, the voltage distributor contains decoupling filters for the two photomultiplier voltages.

(1) Preamplifiers

Originally the preamplifiers had been included in the design of detector circuits in order to make it possible to use short cables at the output of the photomultipliers, to provide a low impedence drive for the coincidence circuit, and to bring the signal level up to the point where it could operate the coincidence circuit effectively. A gain of 30 was adequate for these purposes, and small units with this gain were actually used for some time. It was discovered, however, that pickup from relays in the automatic observer caused spurious counts which could not be eliminated by placing filters in the relay circuits or by a reasonable amount of shielding. Since this pickup originated in the coincidence circuit, it was felt that by increasing the gain of the preamplifiers, the spurious pulses could be overshadowed by feeding in larger signals. By using larger preamplifiers having a gain of 3,000, the effect of such pickup has now been entirely eliminated.

Standard circuits have been used in the design of the preamplifiers. In order to increase signal height, a low capacity cable is used to connect the collector plate of the phototube directly to the input grid of the preamplifier. This cable, the collector plate of the phototube, and the input grid, taken together, have a capacity of about 20 mmf which in parallel with a 10 meg resistor represents the phototube load. Since the current pulse which the phototube passes, as the result of a scintillation lasts about $\frac{1}{4}$ of a microsecond, this load is essentially capacitative.

In as much as the phototube may be thought of as a current

generator, the signal height will be inversely proportional to this capacity. At this stage in the circuit, therefore, the signal will consist of negative pulse rising in $\frac{1}{4}$ of a microsecond and falling off exponentially with the 200 microsecond time constant of the input circuit. After passing through the first two stages of the preamplifier, which together have a gain of 30, the signal passes into an inverter stage which lies in between the first and second feedback loops. The positive signal from this stage then passes into a differentiating circuit having a time constant of 1 microsecond, where the signal becomes a sharp pulse. A differentiating circuit is inserted at this point to avoid blocking of the second two stages of amplification in the preamplifiers, due to pile up of pulses during fast counting. These two stages taken together have a gain of 100 and drive an output cathode follower which is required in order to provide a low impedence drive for the coincidence circuit.

(2) Coincidence Circuit

As was mentioned before, the coincidence circuit takes simultaneous signals from the two phototubes, which look into opposite sides of the scintillation crystal, accepting only those which coincide in time, thereby suppressing most pulses produced by phototube noise which pass through a single channel only. For this application, the requirements on a coincidence circuit turn out to be somewhat different from those encountered in genuine coincidence work. To begin with, there is no necessity for extremely fast resolving time, since the phototube noise consists of relatively few, discrete pulses which rarely coincide

accidentally within the 1.35 microsecond resolving time. Furthermore, resolving times shorter than the scintillation time of the crystal ($\frac{1}{4}\mu$sec) would involve additional difficulties in pulse shaping, since the pulses could not be made shorter than this scintillation time.

A desirable feature for a coincidence circuit to be used in this fashion is high sensitivity to small pulses coupled with a wide acceptance range of pulse heights. High sensitivity is important since the lowest level at which the coincidence circuit should be required to operate lies well into the low region of plentiful noise. Although it is possible to amplify such small signals to the point where they would be capable of operating even a relatively insensitive circuit, additional stages of amplification may be saved by using a very sensitive coincidence circuit, placing it at an earlier point along the chain and thus requiring only a single channel from that point on.

IN34 germanium diodes are used as the non-linear elements in the coincidence circuit which is shown in Fig. 14. Positive pulses having a decay constant of 1.35 μsec are fed into a second set of differentiating circuits designed with precisely the same time constant, so as to avoid a negative return swing from the doubly differentiated signal. These signals are applied to the upper pair of IN34 diodes which constitute the heart of the coincidence circuit.

When a signal appears in a single channel, for example, the upper one, very little of this signal appears on the left hand grid of V1, because for such a signal, the upper diode in back conduction has a much higher impedence than the lower one in forward conduction

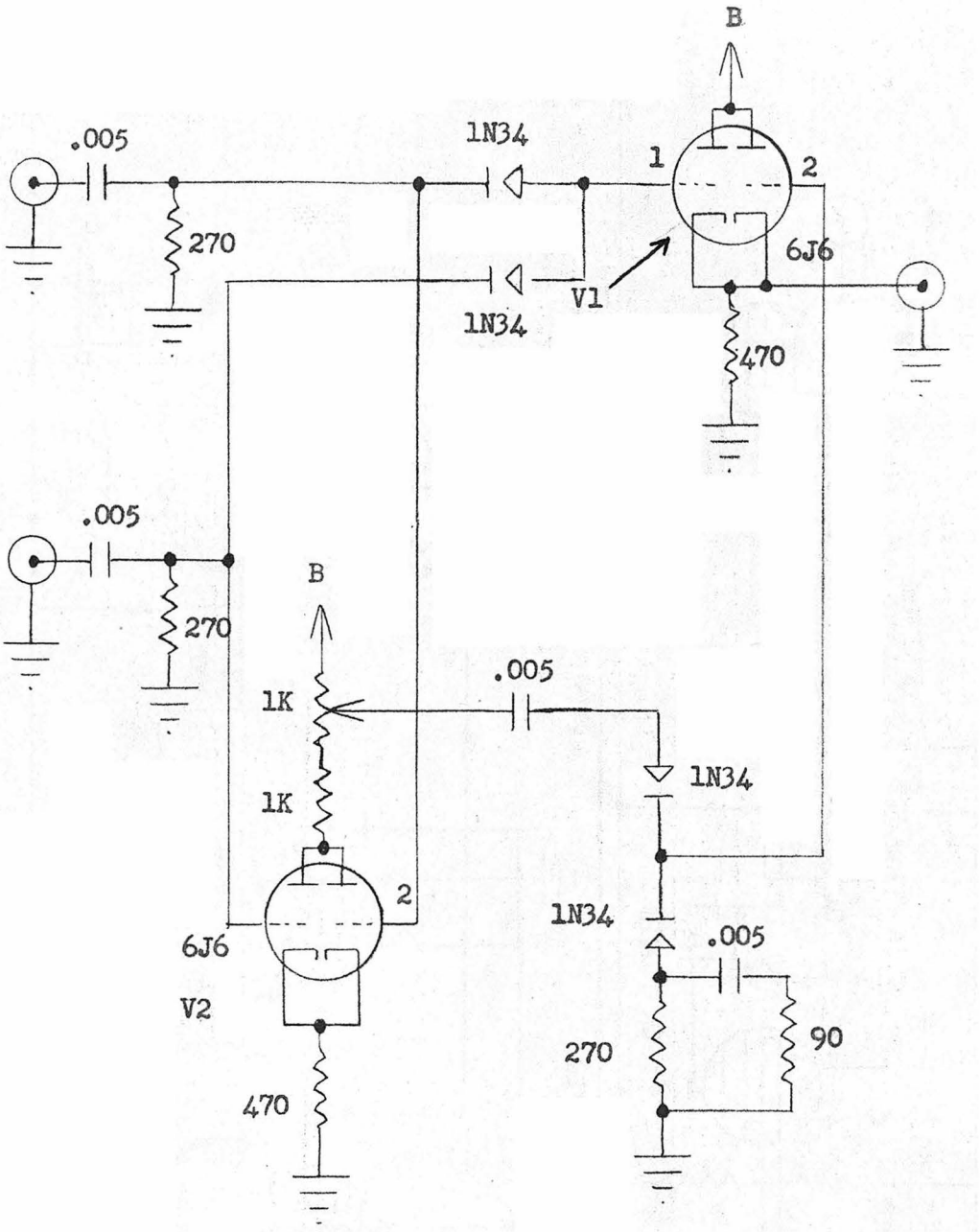

Fig. 14. Balanced coincidence circuit.

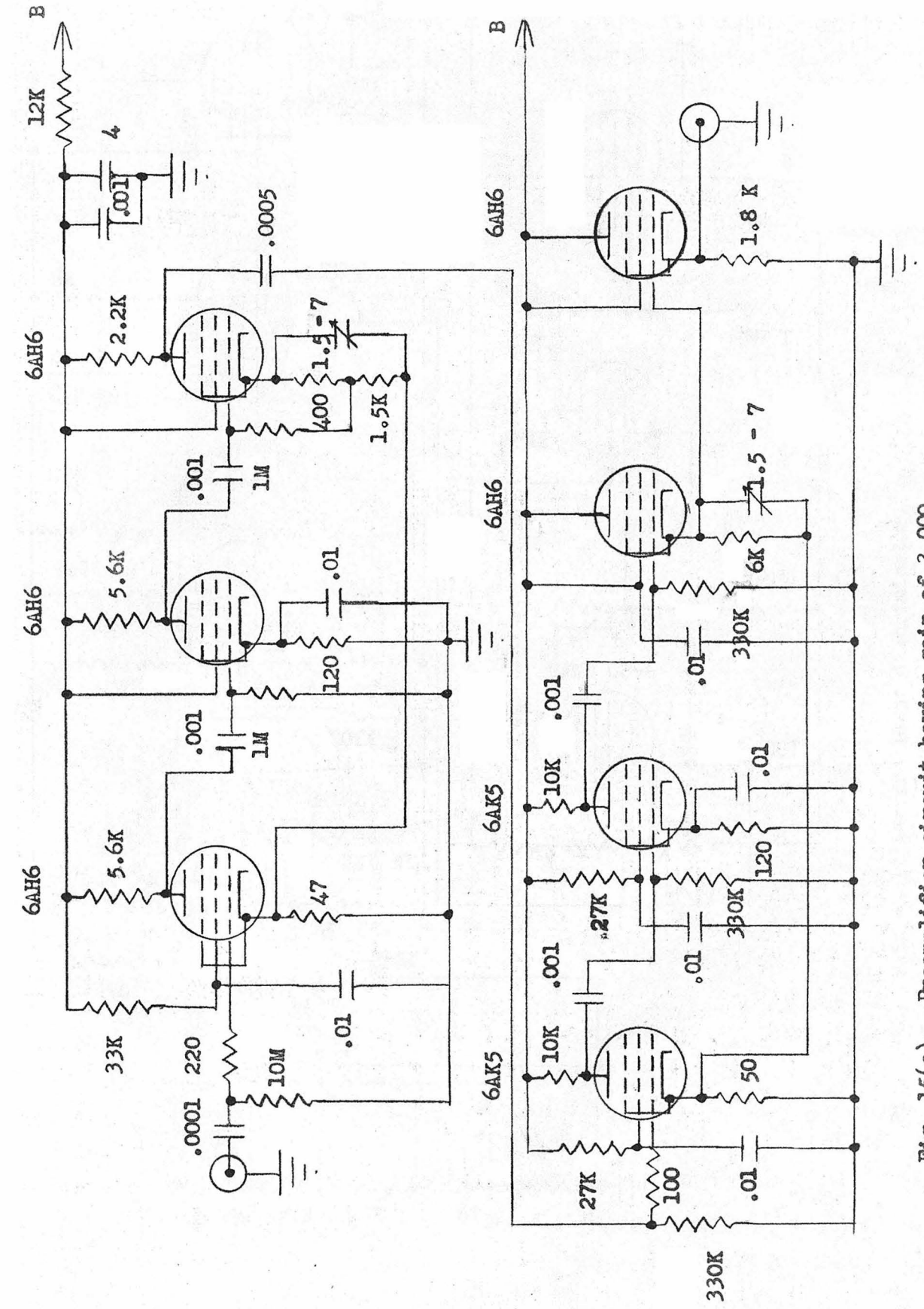

Fig. 15(a). Preamplifier circuit having gain of 3,000.

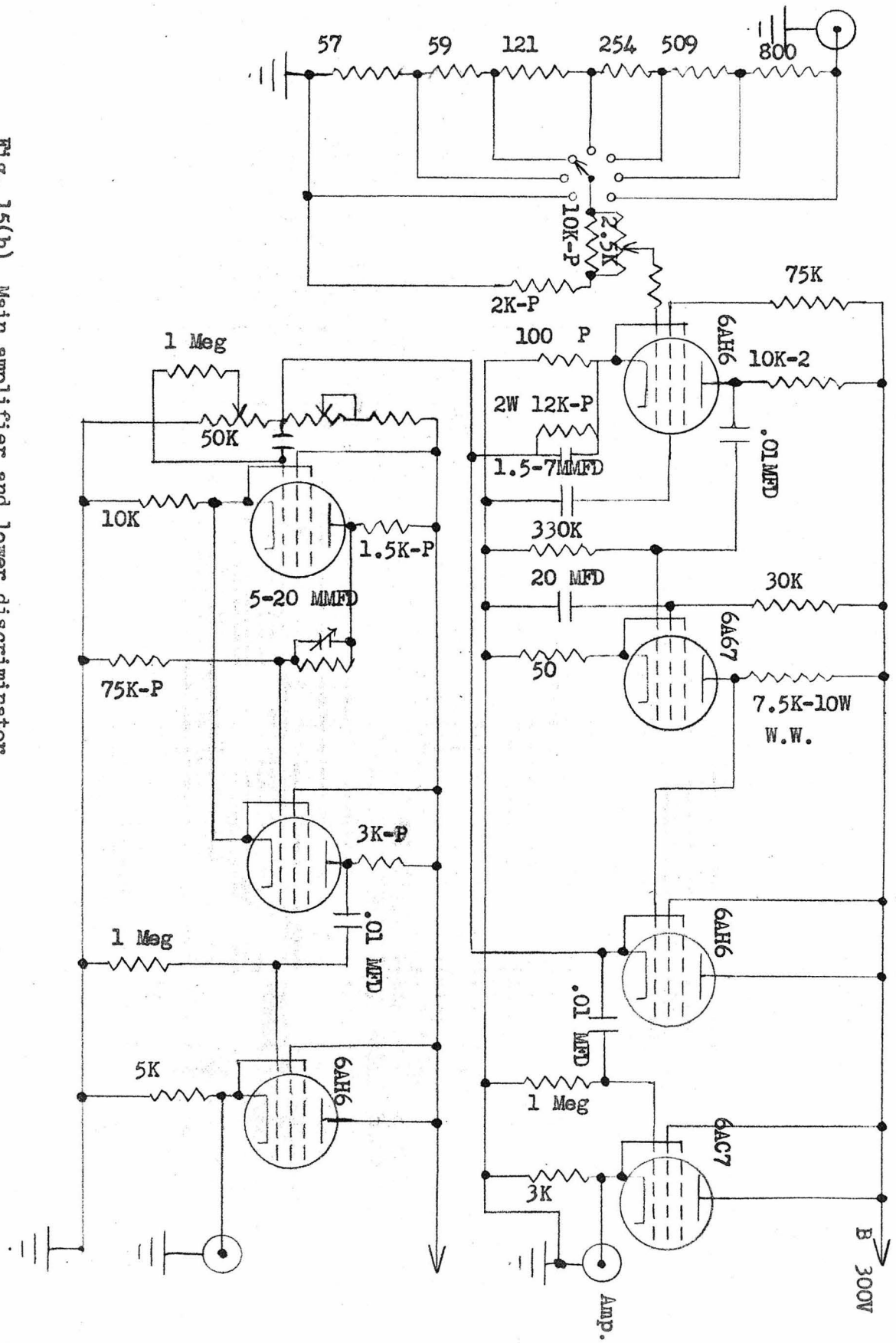

Fig. 15(b) Main amplifier and lower discriminator.

in series with the lower differentiating circuit. On the other hand, when signals appear simultaneously in the two channels, almost the entire signal appears on grid 1 of V1.

It would appear that this much of the circuit alone would be sufficient to provide the proper coincidence action, but it must be remembered that difference between front and back resistance of the diodes becomes quite small as the currents become small. In other words, the non-linear nature of the diodes becomes less pronounced as one investigates a smaller and smaller portion of their characteristic curves. For this reason, it is helpful to cancel out that portion of the signal which would be present if the inputs were mixed linearly, and retain only that part which results from the non-linear characteristics of the coincidence circuit.

Such a cancelling circuit is shown in the lower half of Fig. 14. It is adjusted so as to cancel exactly pulses coming from a single phototube but to fail to cancel coincident pulses from both phototubes because of its linear mixing action. Signals from the differentiating circuits appear on opposite grids of V2, which acts as a linear mixer and inverter. The potentiometer in the plate of V2 should be adjusted so as to provide this stage with a gain of -1 for either of the two inputs. In order to provide the proper attenuation for pulses of all sizes, these signals are fed into a dummy coincidence circuit having only one input, to which is applied the mixture of the two input originals. This dummy coincidence circuit is designed to behave in all respects toward negative pulses as the two upper diodes did toward positives. A differentiating circuit is,

therefore, even placed at the point in the lower circuit where its second input should appear, with a 90 ohm resistor at this point to simulate the output cathode follower in the preamplifier. Negative pulses coming from the dummy coincidence circuit appear on grid 2 of the mixer and output cathode follower V1 where they subtract from the principal signal appearing on grid 1.

Two advantages are obtained from the use of a balanced coincidence circuit of this sort. As was mentioned before, it is possible to avoid amplifying signals from the two phototubes independently to as great an extent as would be necessary if no balancing circuit were used. A second advantage lies in the complete cancellation of large noise pulses arising in a phototube. Such pulses, which occur occasionally, would be likely to get through an unbalanced circuit thus causing a small but significant noise background.

(3) The Main Amplifier

An eight foot cable leads from the coincidence circuit into the main amplifier, which is a modification of a standard amplifier circuit used in many laboratories. It consists of the amplifier proper, a discriminator of the Schmidt trigger type, and a regulated high voltage power supply. The amplifier itself contains only two stages of amplification, including a degenerative feedback loop designed to give it a gain of 100. A stepwise attenuator which can be used to vary the attenuation of the input signal from 1 to 2^{-5} is located at the input. These two stages have a direct output which runs into the scalar and there is applied to the upper discriminator which is

triggered by larger-than-signal pulses. This same signal, coming directly from the two stages of amplification, is also applied to the lower discriminator, which is in the amplifier itself. Its setting can be very precisely adjusted by means of a front panel adjustment so that it will not be triggered by very low level pulses which, for the most part, represent residual noise, but accept practically all true signal pulses. Pulses from the lower discriminator are positive and of uniform height, because of the regenerative trigger action of the circuit. They are fed into the main scalar input.

Upper discriminator and anticoincidence circuits are shown in Fig. 16. A signal from the amplifier is applied to the upper discriminator input at J 1. The discriminator circuit is of the one shot multivibrator type, the duration of the output signal being regulated by the size of C_4. Potentiometer R_4, adjustable on the front panel, is the discriminator bias control which regulates the minimum pulse height required to trigger the multivibrator. This pulse height is equal to the number of volts by which V 1 is maintained below cut off in the stable circuit condition.

A square positive signal lasting 4 microseconds is fed from the plate of V 2 to the left hand grid of V 3 in the anticoincidence circuit, whenever the multivibrator is triggered. This square pulse is used to blot out the main signal coming from the lower discriminator. A complete blotting out is achieved because the one microsecond main signal, which appears at J 2 is delayed by one microsecond in the delay line before being applied to the right hand grid of V 3.

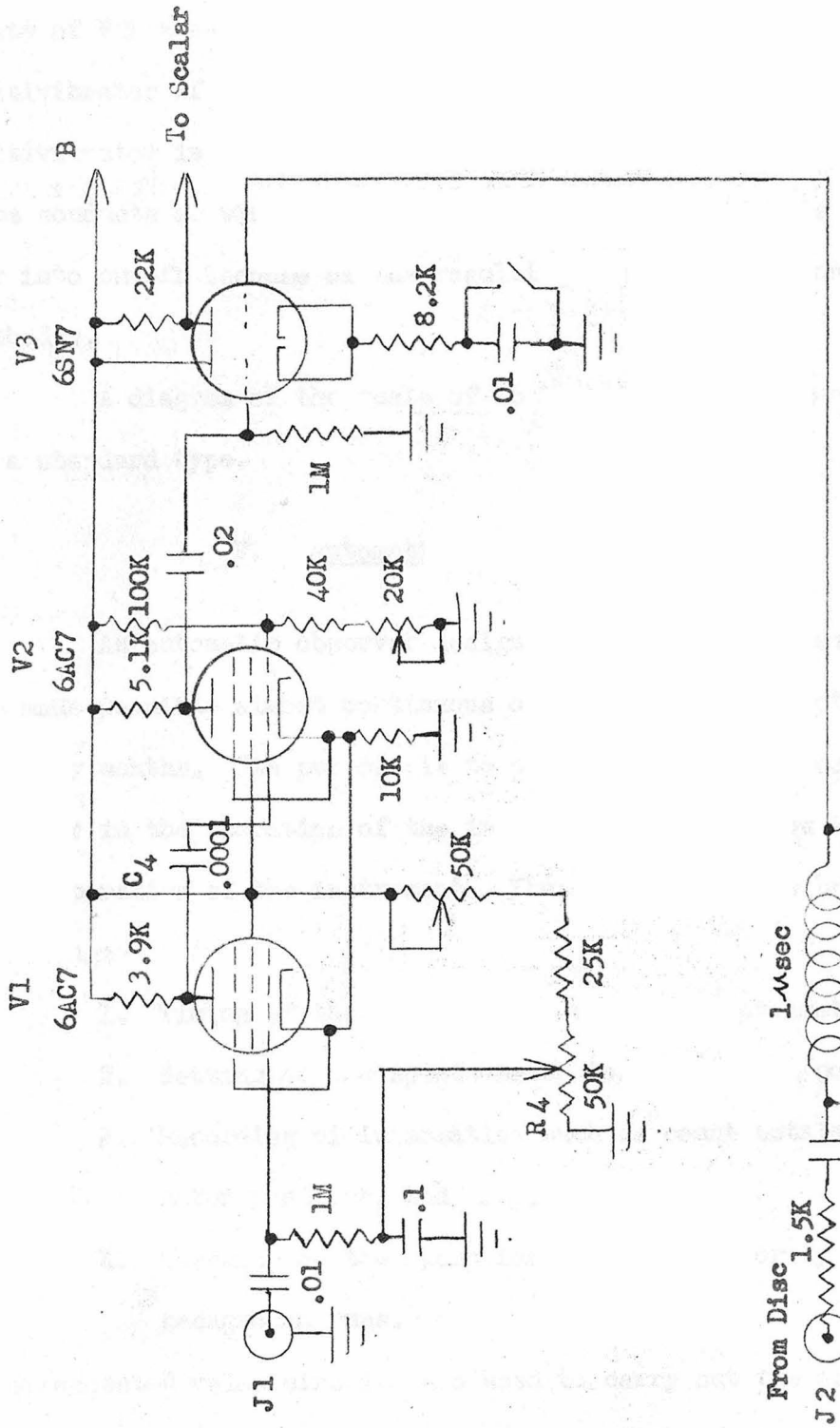

Fig. 16. Upper discrimination and anticoincidence circuit.

No unusual features appear in the anticoincidence circuit, which supplies a negative signal to the scalar from the right hand plate of V 3 whenever the main signal appears on its grid, but the multivibrator of the upper discriminator is not triggered. If the multivibrator is triggered, however, the left hand section of this tube conducts so violently that the right hand section is driven far into cutoff because of the resulting high potential on both cathodes.

A diagram of the scale of 16 is not included since it is of a standard type.

F. Automatic Observer

An automatic observer designed and built by James L. Kohl, has made possible almost continuous operation of the spectrometer for many months. Its purpose is to perform all the duties of a human observer in the operation of the instrument and to allow 24 hour a day operation of the instrument. These functions are briefly the following:

1. Timing of the runs made at various spectrometer settings.
2. Setting of the spectrometer to prearranged positions.
3. Recording of information such as count totals, spectrometer position, and time.
4. Checking on the operation of the detector by means of background runs.

Interconnected relay circuits are used to carry out the above operations. A brief description of the nature of these circuits is included

here.

(1) Timer

The timer supplies the basic rhythm of all operations from its clock, which throws a microswitch every minute causing an additional step forward in the cycle of operations. Runs are timed, therefore, in integral numbers of minutes, the number of minutes in each run being stepped off by a pair of telephone type stepping relays, operating in tandem, so that a complete cycle from the first causes the second to step once. Any number of steps up to ten may be chosen for either of the relays. After each cycle of the first relay, the printer is caused to print; and after each cycle of the second, the spectrometer is moved. Runs lasting anywhere from one to a hundred minutes may therefore be chosen, provided the number of minutes in the run is made up of a pair of factors between one and ten.

Other duties of the timer are: sending control signals to the scalar, printer and wavelength screw set circuits, and providing proper cycling for the counting, resetting, printing, and setting.

(2) Screw Set Mechanism

Programing of a series of runs at different wavelength screw positions is accomplished by use of a punched tape. Holes in this tape may be punched to correspond to desired screw positions for the runs. These holes are felt by a sensitive microswitch, which communicates the information on the tape to the set motor. Accurate setting

of the spectrometer is guaranteed by a precisely machined sector wheel attached to the spectrometer screw, which contains 50 equally spaced plastic insulated sections separated by 50 grounded brass conducting sections. A contact riding on this sector wheel makes and breaks connections which determine the exact set position of the spectrometer. The holes in the punched tape choose the particular sector at which the screw will stop. By means of this arrangement, no reliance need be placed upon the accuracy with which holes are punched in the tape.

(3) Additional Parts of the Robot Observer

Record is kept of count totals and subtotals of the counts in each run as well as the screw position. The screw position is transmitted to the printing unit by means of a selsyn indicator whose operation is quite independent of the programming tape mechanism. Time is also recorded with each print to make possible corrections for the decay of short lived sources and to provide an additional check upon the operation of the equipment. Important data not recorded automatically are the temperature of the crystal and tilt (level) of the source. By means of the robot control, a lead shutter 8" thick is periodically made to intercept the beam of gamma rays to allow a check upon the background counting rate of the detector. After a predetermined number of runs have been taken, a background run of this type is interjected. The frequency of the background runs is adjustable on the front panel. Such a background run lasts as long as the other runs, but the screw position does not change before it occurs.

Therefore, no points are skipped in the line profile.

II. ANALYSIS OF ERRORS IN WAVELENGTH MEASUREMENTS

A. Calibration of the Spectrometer

Because of the mechanical complexity of the curved crystal spectrometer and the many operations involved in the determination of gamma ray and x-ray wavelengths, any treatment of precision is inevitably quite complex and difficult. Nevertheless, such a treatment is necessary for a proper evaluation of results, and therefore, it will be attempted in this section.

In order to facilitate this treatment, errors will be thought of as being of two types. The first type will include errors resulting from lack of mechanical precision in the instrument and errors in its calibration. The second type will include errors produced by statistical variations in counting and errors arising during the reduction of the data.

Errors of the first type, which in most cases seem to be the dominant ones are also the least subject to mathematical treatment. In order to indicate how these errors appear, a condensed description of the entire calibration procedure will be presented here.

An absolute calibration of the instrument is obtained by using the $K\alpha_1$ x-ray line of tungsten as a standard. Its wavelength has recently been measured with high precision at this laboratory by W.J. West, using a double crystal spectrometer[13]. West's value for this wavelength is 208.575 ± 0.008 x.u. This line lies within the range of the curved crystal spectrometer and has been run by Watson[13],

and later by others, using a tungsten target x-ray tube behind a slit placed in the position of the usual source. A known reference position on the wavelength scale is obtained in this way and all further calibrations thus are made relative to this standard. Typical profiles for this line are shown in Fig. 17. West's measurement may be converted from Siegbahn x-units to milliangstroms by use of the conversion ratio $\lambda_g/\lambda_s = 1.002024$ recently obtained by DuMond and Cohen[14], giving 208.996 milliangstroms for this wavelength.

A temperature correction should be applied to all gamma ray measurements, but this correction only becomes significant in the measurements of long wavelengths and for this reason, is omitted with medium and short wavelengths. To apply this correction, one assumes that the principal metallic parts of the spectrometer expand and contract in constant proportion, so that no angles will be altered by such motion. Wavelengths will then be proportional to the spacing of the quartz (310) planes which provide selective reflection. A thermal expansion coefficient of 14.5×10^{-6} per degree C is used in this correction.

Since the source is moved with respect to the crystal by means of a sine screw, the wavelength setting of the spectrometer, which is proportional to the sine of the angle of incidence, may be expected to be a linear function of screw position. An extensive calibration of the deviations from linearity of the screw has been carried out with a microscope and standard decimeter scale as follows:

The glass scale, which had been calibrated by the National Bureau of Standards was mounted on the carriage carrying the source

TUNGSTEN K α_1 X-RAY LINE

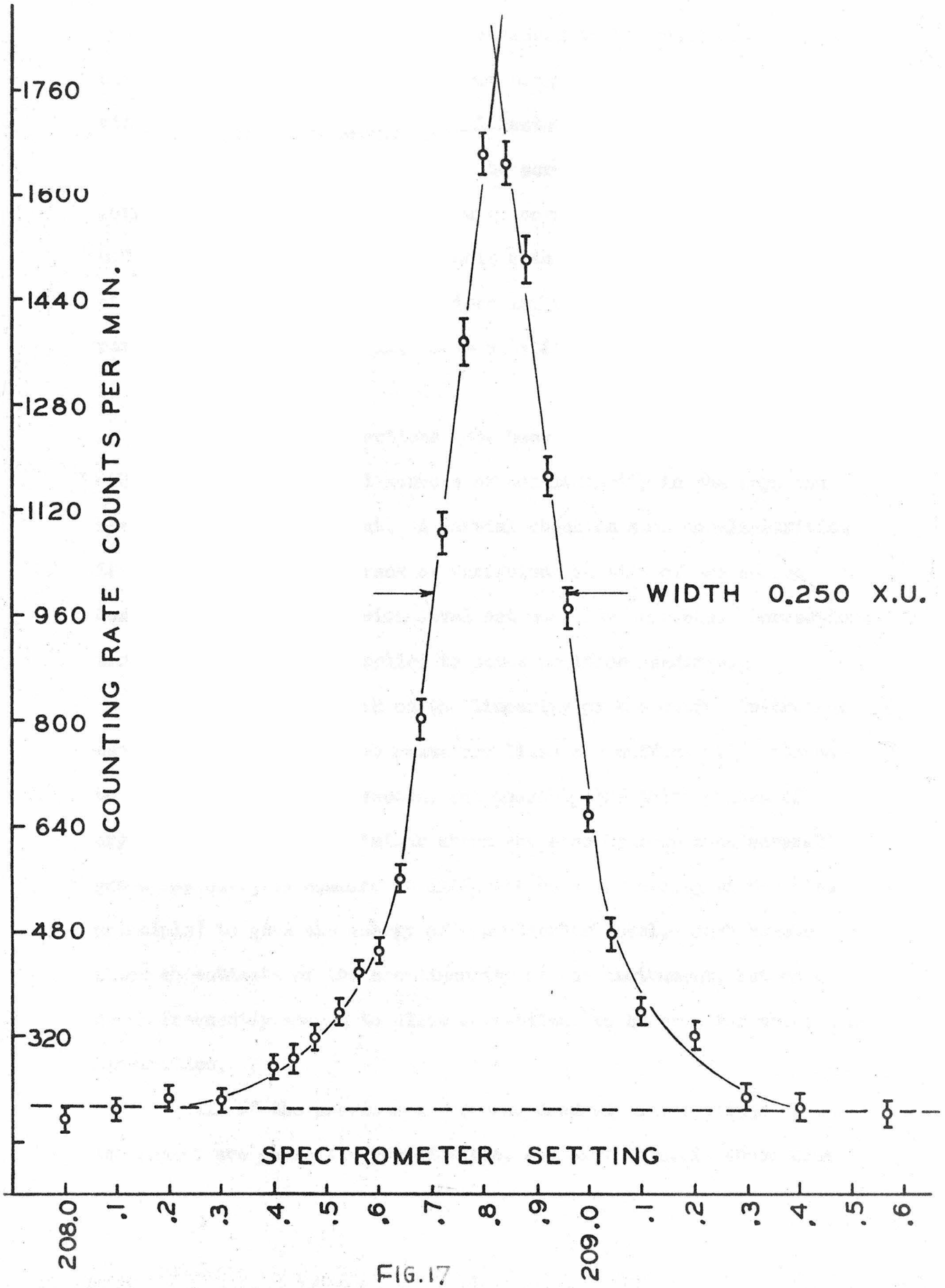

FIG.17

beam. A 100 power microscope was attached to the middle carriage carrying the precision screw. Screw positions were noted every 5 millimeters over a range of 600 millimeters, a millimeter per revolution being roughly the pitch of the screw. In addition to this long range calibration, a short range correction to screw position had to be applied which was periodic with respect to the revolution of the screw. The extensive calibration with the periodic error removed is shown in Fig. 18, while a typical periodic correction is shown in Fig. 19.

After such corrections have been made, there still remain other possible mechanical sources of non-linearity in the ways and bearings of the instrument. A partial check on such non-linearities is obtained by keeping track of variations in tilt of the source bomb by means of a precision level set upon its carriage. Corrections for this tilt are then applied to screw position readings.

An absolute check on the linearity of the entire instrument can sometimes be made when gamma ray lines are sufficiently intense to be obtainable in the second, and possibly the third orders of crystal reflection. A similar check may also be made when several gamma ray energies combine in different ways (according to the Ritz principle) to give the energy of a particular level. Such checks allow an estimate of the non-linearity of the instrument, but do not occur frequently enough to allow corrections to be made for these non-linearities.

All of the previous discussion assumes that settings of the instrument are perfectly reproducible, and therefore, if these non-

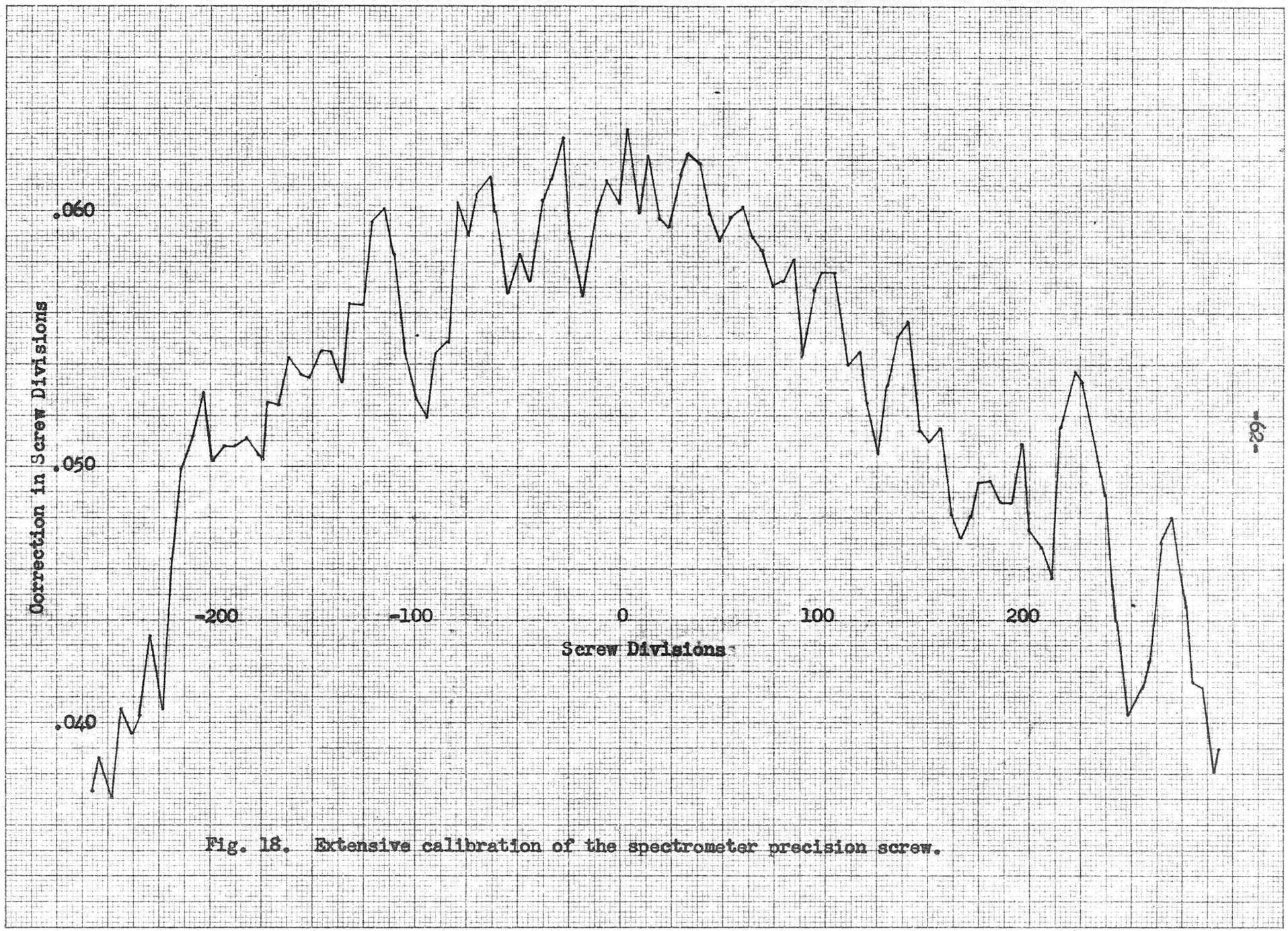

Fig. 18. Extensive calibration of the spectrometer precision screw.

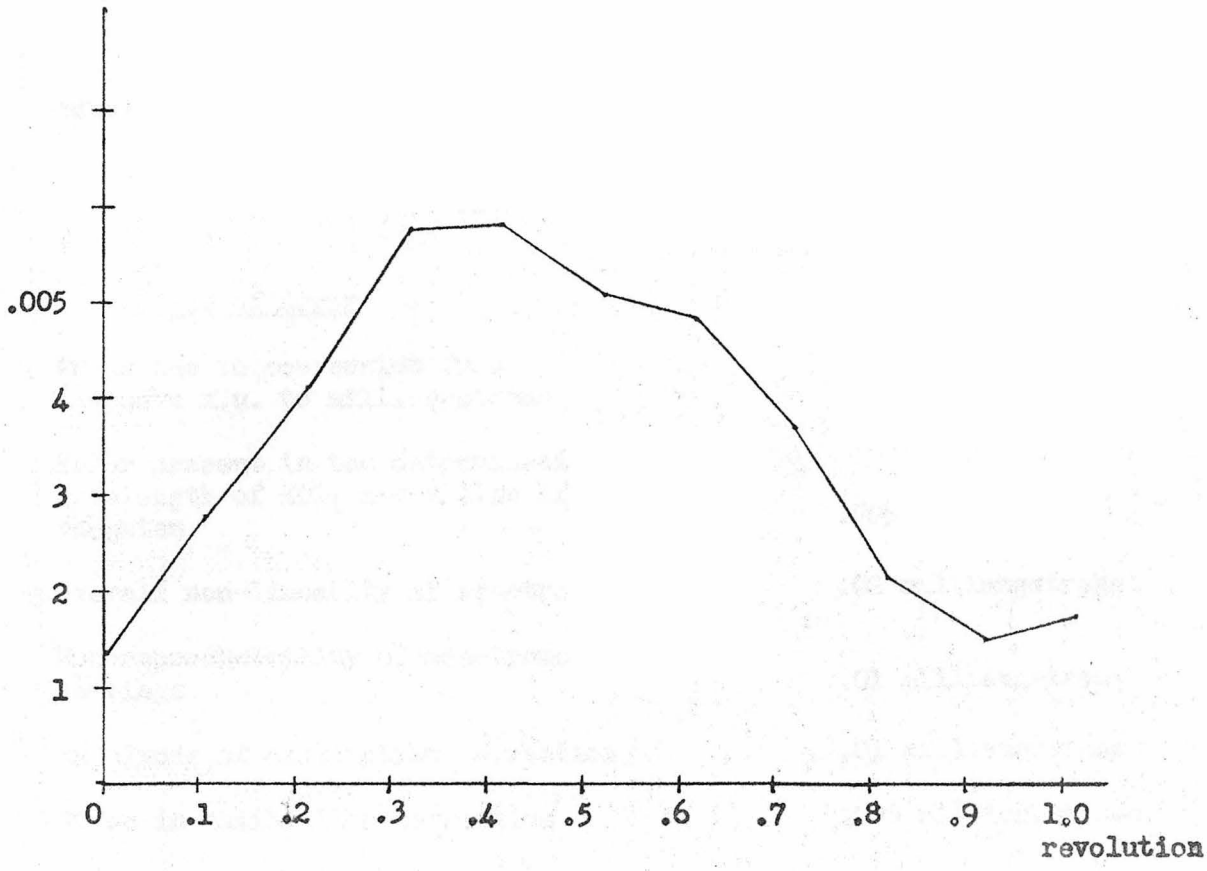

Fig. 19. A typical periodic correction of the precision screw over one revolution.

linearities were well known, the measurements could be corrected. This assumption is not entirely true, however, since repeated measurements of wavelength sometimes indicate a small but definite hysteresis in the mechanism.

Estimated relative magnitudes of the errors involved in wavelength measurements are presented in the following table.

Table I

Cause of Error	Rough Magnitude of Error
Error due to conversion from Siegbahn x.u. to milliangstroms	.001%
Error present in the determination of wavelength of $K\alpha_1$ x-ray line of tungsten	.005%
Overall non-linearity of spectrometer	.02 milliangstroms
Non-reproducibility of spectrometer settings	.01 milliangstroms
Magnitude of calibration correction	.01 milliangstroms
Error in calibration correction	.003 milliangstroms
Error produced by statistical variations in counting	.001 milliangstroms
Error arising during reduction of data	.002 milliangstroms

B. Errors in Wavelength Measurement Produced by Statistical Variations in Counting Rate

A semi-quantitative treatment of those errors in wavelength measurement which result from statistical variations of counting rate is possible and will be presented in the next section. In order to work out the theory of such errors, it is necessary to understand the

process by which data are reduced and final measurements obtained.

For each wavelength measurement two peaks are obtained. One peak is taken using internal reflection from one side of the crystal planes, while the other peak is taken using internal reflection from the opposite side. The shape of such a line profile represents the fold of the intensity distribution of the source, and the "window curve" of the crystal*, as well as the spectral shape of the line being investigated. In the case of gamma radiation, spectral width is generally quite negligible compared to instrumental width, so that the shape of the profile is quite independent of the former.

Plotted on a wavelength scale, such a profile resulting from source and crystal "windows" alone will have a shape and breadth which is independent of the wavelength being measured. It is interesting to note that asymmetries in the source or crystal windows are properly repeated in both left and right hand reflected profiles corresponding to a given line, while asymmetries in spectral shape of the line are mirrored when one passes to the second profile, thus providing a valid criterion for distinguishing true structure from source irregularities and inaccurate crystal focusing.

A preliminary plot is first made of the line profiles. The background counting rate appearing on either side of the line profile is then subtracted from all the points on a line. Generally, this

---

* By "window-curve" of the crystal is meant the plot of reflectivity versus angle of incidence taken over the small angular variation within which selective reflection occurs.

background is the same on either side of the line but in certain cases the background changes rapidly enough so that a linear correction must be subtracted from the points. Such a rapid variation in background occurs near the central position of spectrometer where scattered radiation from the collimator accounts for most of the background, or in the "tail" of a second line adjacent to the first which is much more intense than the one under investigation.

Wavelengths may be determined from the distance, as measured on the sine screw between two profiles. In order to determine this distance as accurately as possible using existing data, a procedure has been worked out which is designed to make the best possible use of all points.

For this purpose, a composite curve is constructed on tracing paper from all lines in the spectrum of a particular source after they have been normalized to the same height. Profiles from the same source should all have the same shape, provided the spectral widths of the lines are negligible. This composite curve is then superposed upon each profile in turn so as to give what visually seems to be the best fit. Wavelength is taken as proportional to the sine screw distance between the best fittings of the composite curve upon two opposite profiles corresponding to a certain line. A composite profile of this type used with a source of iridium 192 is shown in Fig. 20. Fitting the profile to each line is, of course, somewhat a matter of personal judgement; but since it is a very simple procedure, it may be repeated by several people and an estimate of the human error may be made.

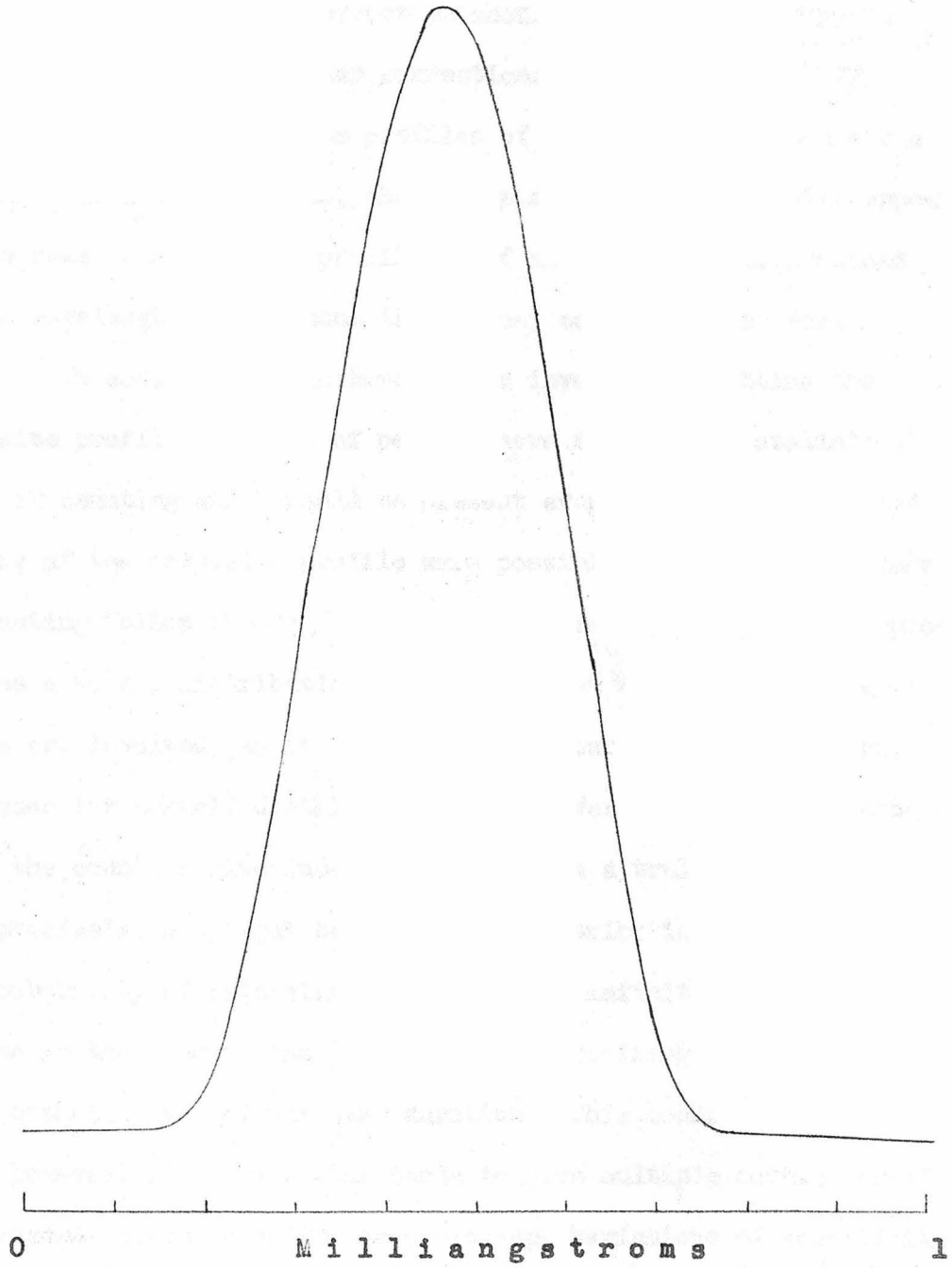

Fig. 20. The composite line profile used with the source of iridium 192.

It is important to note here that sources having short half-lives decay appreciably while any one line profile is being explored. Consequently, correction should be made for decay, in addition to the various other corrections described above. If, however, successive opposite profiles of a particular line are run for the same length of time, the asymmetry in line shape will appear in the same sense on both profiles, and no error will be produced in the wavelength measurement if no decay correction is made.

In addition to the human error involved in fitting the composite profile to a set of peaks, there remains the statistical error of counting which would be present even if a "least squares" fitting of the composite profile were possible. Statistical errors of counting follow the well known Poisson distribution, which approximates a normal distribution quite well when a hundred or more counts are involved, as is the case in all our applications here. A Poisson (or normal) distribution is, however, only obtained provided the counts arrive independently and in a truly random fashion. More precisely, one might say that this distribution is obtained if the probability of obtaining a count in any infinitesimal interval of time is the same as the probability of obtaining a count in any other such interval of the same duration. This condition will not hold, however, if the detector tends to give multiple counts, or if the detector circuits suffer from pick-up, variations of sensitivity with time, or certain other troubles. Such difficulties may often be detected most easily by checking the randomness of counting, using a χ^2 test.

In this way, a very delicate and truly significant test on the operation of the counter may be performed, and if the test shows no trouble is present, the analysis of error, which is based on the assumption of randomness will be justified. A typical test of this sort is given here as an example. Twenty counting intervals of one minute each were used.

Number of interval	Number of counts recorded
1	356
2	357
3	323
4	322
5	361
6	346
7	340
8	342
9	338
10	345
11	342
12	352
13	365
14	372
15	327
16	326
17	332
18	338
19	331
20	368
Av.	344.15

Let n_i represent the number of counts in the interval i. In this example, $\chi^2 = \frac{\sum(n_i - 344.15)^2}{344.15} = 12.85$, and nineteen degrees of freedom are present. By use of statistical tables, one finds that the probability of a purely random sample showing greater variation is 0.85. Deviations from randomness in this case, if present at all, are certainly too small to be of any importance. In other cases,

however, tests of this sort have pointed out the existence of troubles in the detector and its electrical circuits by indicating significant deviations from random behavior.

Let us assume proper behavior of the detector, and ask ourselves what error in wavelength may be expected as a result of the statistical variations in counting. Such a question can be answered only by a thorough consideration of the effect of small variations in the positions of points forming a line profile, upon the "best fit" of the composite profile to this line. Let $L(\lambda)$ be the number of counts per minute to be expected at a certain wavelength setting of the screw λ. $L(\lambda)$ considered as a function, therefore, represents the true line profile. If we take a series of runs lasting τ minutes each at a set of positions λ_i, $i = 1, \cdots n$, the expected number of counts at each point will then be given by $\tau L(\lambda_i)$, and the standard variation of each such point from its expected number of counts will be $\sqrt{\tau L(\lambda_i)}$, in accordance with the extension of the Poisson distribution to the normal distribution. Each run at a point λ_i may be thought of as constituting an independent measurement of the position of the composite profile, since the profile, once obtained, could conceivably be fitted to a single point. As such, the standard error of the position measurement corresponding to a run at λ_i lasting τ minutes is $\sqrt{\tau L(\lambda_i)}/\tau L'(\lambda_i)$, provided that the slope $L'(\lambda_i)$ of the curve $L(\lambda_i)$ does not change appreciably over the vertical interval $\sqrt{\tau L(\lambda_i)}$, so that the error in fitting the composite profile horizontally may also be considered normal. The combined effect of the runs on all n points can be regarded

as a combination of independent measurements, each contributing with a weight inversely proportional to the square of its standard error. Hence, if $\mathcal{E}$ is the standard error of the fitting of the composite profile to all points, we obtain

$$\frac{1}{\mathcal{E}^2} = P = \sum_{i=1}^{n} \left(\frac{\tau L'(\lambda_i)}{\sqrt{\tau L(\lambda_i)}} \right)^2 = \sum_{i=1}^{n} \frac{\tau (L'(\lambda_i))^2}{L(\lambda_i)} \qquad (1)$$

The quantity $P = \mathcal{E}^{-2}$ is a convenient measure of the precision of fit. If the points λ_i are rather closely spaced, one would expect no large change in P to result from the assumption that they are everywhere dense, provided the length of time $n\tau = T$ to pass over all the points remains constant while n increases. For convenience, we shall also take them as being equally spaced. These assumptions clearly allow us to convert the sum in equation 1 into an integral. Take $W = \lambda_n - \lambda_1$ as the total interval covered in going across the line and take $\Delta\lambda = \lambda_{i+1} - \lambda_i$ as the spacing of points in this interval. Then $\Delta\lambda = W/n$, so

$$P = \sum_{i=1}^{n} \frac{\tau n}{W} \frac{L'(\lambda_i)^2}{L(\lambda_i)} \Delta\lambda$$

or

$$P = \sum_{i=1}^{n} \frac{T}{W} \frac{L'(\lambda_i)^2}{L(\lambda_i)} \Delta\lambda$$

If we let n increase indefinitely, holding T and W fixed, while $\Delta\lambda \longrightarrow d\lambda$, we obtain

$$\lim_{n\to\infty} P = P_\infty = \frac{T}{W} \int \frac{[L'(\lambda)]^2}{L(\lambda)}\, d\lambda \qquad (2)$$

where the integration is taken over the region of λ being investigated. It is interesting to note that W/T = R is the rate at which the line is traversed. In other words, $W/T = R = \frac{d\lambda}{dt}$, where dt is an infinitesimal interval of time. Upon substituting this expression into equation 2, there results

$$P_\infty = \int \frac{L'(\lambda)^2}{L(\lambda)}\, dt \qquad (3)$$

which is somewhat more general in that it remains true even if the interval is not traversed at a uniform rate. In summary, it should be pointed out that formulae 2 and 3 were derived by use of the following approximations.

1. All counting intervals contain enough counts so that the Poisson distribution may be approximated by a normal distribution.

2. All errors are small enough so that, within their range, the curve $L(\lambda)$ does not change slope appreciably.

3. Points on the profile are sufficiently closely spaced so that a continuous distribution of points may be used to approximate the actual discrete distribution.

Of these three assumptions, number 2 is the most serious one since it tends to break down in the case of lines which are so weak as to be barely detectable. Without use of assumption 2, however, the development of the theory would be extremely difficult.

In order to permit an actual calculation of error, some assumption must be made concerning the shape of the line profile $L(\lambda)$. To the three assumptions above we therefore add a fourth.

4. The line profile has the shape of an isosceles triangle, its apex representing the line peak, and the extended background representing its base.

This simple profile seems to be very nearly the shape of the actual one in many cases (see Fig. 20), and certainly is not so far wrong as to cause a greatly incorrect estimate of P. Let us therefore take the peak height as H, above the background B, and the base width as W. Also let us change the independent variable from λ to $\ell = \lambda - \lambda_1$, so that in the region under consideration $0 \leqslant \ell \leqslant W$. Then $L(\lambda) = H\, f(\ell) + B$

where $f(\ell) = \frac{2}{W}\ell$ when $0 \leqslant \ell \leqslant \frac{1}{2}W$

and $f(\ell) = 2 - \frac{2}{W}\ell$ when $\frac{1}{2}W \leqslant \ell \leqslant W$

Upon differentiating $L(\lambda)$, we obtain

$$L'(\lambda) = H\, f'(\ell) = \frac{+2H}{W} \qquad 0 \leqslant \ell \leqslant \tfrac{1}{2}W$$

$$- \frac{2H}{W} \qquad \tfrac{1}{2}W \leqslant \ell \leqslant W$$

giving $\left[L'(\lambda)\right]^2 = \frac{4H^2}{W^2}$ $\qquad 0 \leqslant \ell \leqslant W$

Substituting these results into equation 2, we obtain

$$P_\infty = \frac{T}{W}\int_0^{\frac{W}{2}} \frac{\frac{4H^2}{W^2}}{\frac{2H}{W} + B}\, d\ell + \frac{T}{W}\int_{\frac{W}{2}}^{W} \frac{\frac{4H^2}{W^2}\, d\ell}{(2 - \frac{2}{W}) + B}$$

$$= \frac{2T}{W}\int_0^{\frac{W}{2}} \frac{\frac{2H}{W}\, d\ell}{\ell + \frac{BW}{2H}}$$

giving finally

$$P_\infty = \frac{4HT}{W^2} \log \frac{H+B}{B} \qquad (4)$$

When using this formula it must be remembered that the wavelength is obtained by taking the difference between two opposite adjustments of the composite profile, so the precision of the actual measurement of wavelength is cut in half. Furthermore, the time actually spent in the determination is thereby doubled, and if, in addition to this, one allows half the time for a determination of the background, one obtains 4T for the total time. On the other hand, the distance between opposite peaks, as measured in screw divisions, is very nearly twice the wavelength and consequently a factor of 2 is inserted into W measured in screw divisions, if $\mathcal{E} = P^{-\frac{1}{2}}$ is desired in milliangstroms. As a typical example of a rather weak and broad line, let us take H = B = 300 counts/min., let W = 0.5 screw divisions, and let the total length of the run be 20 hours so that

T = 5 hrs. = 300 minutes. In this case, Eq. 4 yields

$$P_{\infty} = \frac{2 \times 4 \times 300 \times 300}{(0.5)^2} \log 2$$

$$= 2 \times 10^6 \text{ (milliangstroms)}^{-2}$$

The standard error of the wavelength due to statistical fluctuations alone is therefore

$$\mathcal{E} = \frac{1}{\sqrt{P_{\infty}}} = 0.7 \times 10^{-3} \text{ milliangstroms}$$

This example shows, as previously asserted, that errors from this source are much smaller than instrumental errors.

Formula 1 might conceivably be used to determine an optimum spacing of points λ_i. It certainly seems unlikely that uniformly distributed points should give maximum precision. In this case, however, it is clear that the result obtained from formula 1 is not satisfactory since, in order to maximize P by formula 1, the run should be made entirely on a single point on the profile λ_m at which $\frac{[L'(\lambda_m)]^2}{L(\lambda_m)}$ has its maximum value. There are three principal objections to following this procedure.

1. By taking only a single point, a very convenient check on the operation of the detector, as well as the rest of the instrument, has been lost. This check is obtained by comparing the shape of the line profile with the composite profile to which it should correspond closely if the equipment is operating properly.

2. One would be unable to normalize a single point to unit

line height and so it would be impossible to fit the composite profile.

3. It is just as important to determine carefully variations in background in the neighborhood of a line, as to explore the line itself, since a sloping background will materially displace the position of the peak.

It must be concluded, therefore, that the distribution of points should be decided upon the basis of other considerations as well as calculated precision alone, and a uniform distribution seems to be a suitable compromise.

Formula 4, however, may be used to determine optimum settings for the upper and lower discriminators. Let $h(x)$ represent the differential spectrum of the line in question, such as the one shown in Fig. 11. Let $b(x)$ represent the differential spectrum of background. A spectrum $b(x)$ of irreducible background is shown in Fig. 21. Let x_1 and x_2 be the settings of the lower and upper discriminators respectively. Then $H = \int_{x_1}^{x_2} h(x)\,dx$ and $B = \int_{x_1}^{x_2} b(x)dx$. Settings x_1 and x_2 should be made so as to maximize the quantity $H \log \frac{H+B}{B}$ appearing in the expression for P_∞. Since these settings are only important in the case of weak lines, we shall consider only the case of $H << B$. In this case, the quantity $H \log \frac{H+B}{B}$ approaches H^2/B which may be maximized quite easily; its maximum value occurring when

$$\frac{h(x_1)}{b(x_1)} = \frac{h(x_2)}{b(x_2)} = \frac{H(x_1, x_2)}{2B(x_1, x_2)} \qquad (5)$$

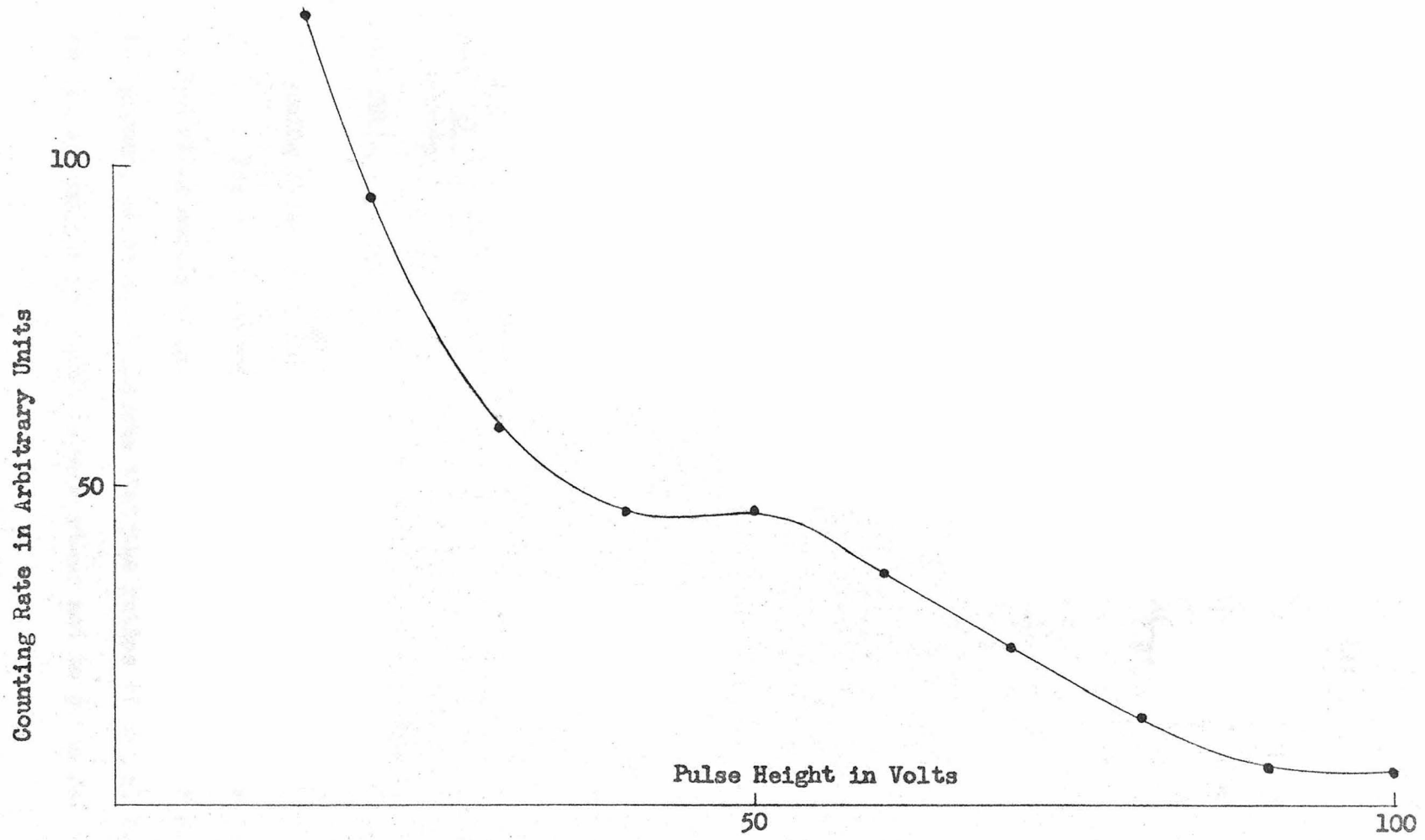

Fig. 21. Differential pulse height distribution of irreducible background taken using a 7.5 volt differential window. The end point of a cobalt 60 distribution appears at 90 volts on this scale.

One may obtain this result by remembering that

$$\frac{\partial H}{\partial x_1} = \frac{\partial}{\partial x_1}\left(\int_{x_1}^{x_2} h(x)dx\right) = -h(x_1)$$

and $$\frac{\partial H}{\partial x_2} = \frac{\partial}{\partial x_2}\left(\int_{x_1}^{x_2} h(x)dx\right) = h(x_2)$$

similarly $$\frac{\partial B}{\partial x_1} = -b(x_1)$$

and $$\frac{\partial B}{\partial x_2} = b(x_2)$$

To maximize $$\frac{H^2}{B}$$

we set $$\frac{\partial}{\partial x_1}\left(\frac{H^2}{B}\right) = 0$$

so $2Bh(x_1) = Hb(x_1)$

and $$\frac{\partial}{\partial x_2}\left(\frac{H^2}{B}\right) = 0$$

so $2Bh(x_2) = Hb(x_2)$

Combining these two results, we obtain Eq. 5.

The criterion expressed by Eq. 5 may be approximately fulfilled after merely inspecting the differential curves of signal and background, since Eq. 5 asserts that the ratios of signal to background at the end points are equal to each other and to $\frac{1}{2}$ the ratio of areas

lying between these end points. Conveniently enough, the differential curves of signal and background do not have to be plotted to an absolute scale, or even to the same scale, since only the ratios are involved. In this way, one is able to use direct radiation from the source to determine the differential curve h(x) and, combining it with the known curve b(x), obtain quickly the proper discriminator settings.

The above procedure cannot be carried out so easily when the principal background is due to the presence of the source. This background is produced, to a small extent, by penetration of the source and detector shielding by direct radiation from the source and, to a much larger extent, by radiation scattered from the quartz crystal and the sides of the collimator. Background from the source becomes important whenever much stronger lines than the ones being investigated are present in the source or whenever quite high energy lines are being studied. Otherwise, irreducible background becomes the principal consideration.

An interesting modification of the present scheme might be made by weighting pulses of different heights different amounts when the final count is totaled. It seems natural that in regions of the pulse height spectrum, where the signal-to-background ratio is high, the pulses should receive more weight than in other regions. To carry this out would, of course, require the use of a multichannel discriminator to accomplish the separation of pulses and therefore would involve large expenditures in time and equipment, which hardly seem justified by the advantage to be achieved.

C. Causes of Line Breadth

As mentioned in the previous section, the characteristic shape of a line profile is determined almost entirely, in the case of gamma rays, by the shape of the source and the focal window profile of the crystal. It is desirable to narrow this profile as much as possible, since by doing so one increases the precision obtainable in a given period of time. Although this fact seems quite evident intuitively, it can also be inferred from formula 4, which has W^2 (W is the base width of the profile) in the denominator of the expression for P_{oo}. Another advantage to be gained by narrowing the instrumental width is an increased ability to resolve closely spaced multiplets. Although such multiplets occur rarely in gamma spectra, they have been discovered in the spectra of iridium 192 and radiothorium[15] and may perhaps be revealed in other spectra when they are scrutinized with a high resolution instrument.

Aberrations of the curved crystal have been extensively discussed in the literature[2,3,4]. Significant broadening of the crystal window has been shown to result from two main causes:

1. Geometrical breadth due to accidental deviations of the stressed crystal from a true cylinder.

2. Breadth resulting from the natural diffraction pattern of the stressed crystal.

Other aberrations of the crystal contribute to a lesser extent and will not be discussed here. The first effect prevents the projections of the crystal planes, which are perpendicular to the

crystal face, from intersecting in a common line thus producing a corresponding breadth of the focal spot. This effect has been minimized by the use of a precision method for grinding cylindrical surfaces upon the steel blocks used for clamping the quartz crystal[16]. Use of this method, combined with careful lapping and clamping, has produced intersection of the projected crystal planes to within 0.05 mm in 2 meters.

Tests using x-rays, similar to the Hartmann test in optics, are used to determine how accurately rays from various portions of the crystal converge. These tests are described in detail in the theses of Lind, Brown, and Klein as well as in the original article describing the spectrometer[2,4,5,12]. They make possible an estimation of the relative importance of the two crystal effects which contribute to line breadth. The results are as follows:

1. X-ray Hartmann tests indicate that the crystal planes converge to within 0.05 mm at the focus.

2. Total crystal breadth amounts to 0.15 mm at half maximum. This result was obtained by using an extremely narrow source of gold 198 (0.001 inches thick) which has a gamma ray at 411 kev. Essentially, no contribution to the line profile came from the source in this case, so that the profile itself could be regarded as the crystal window.

The intrinsic diffraction pattern of the crystal, therefore, is the main contributor to the width of the crystal window, since it is of the order of 0.15 mm. This fact is confirmed by the observation that no appreciable change in line breadth is obtained by using only

small portions of the crystal or the source and masking the unused portions with lead.

It should be mentioned that this natural breadth of the diffraction pattern of the stressed crystal is roughly four times the breadth obtained with the same crystal when it is unstressed and used in the double crystal spectrometer[3]. Furthermore, the breadth obtained with a 2 mm thick stressed crystal appears to be approximately double that obtained with a 1 mm thick stressed crystal. No explanation for these anomalies has yet been obtained[3].

An understanding of the behavior of the crystal enables one to choose an optimum source shape and crystal thickness for various situations. To begin with, one must distinguish between two cases.

Case 1. The wavelength of the gamma ray under consideration is known with sufficient accuracy to permit location of the line profile with very little searching.

Case 2. The wavelength of the line is initially unknown so that most of the time is spent in locating the screw position corresponding to the line and, once this position is located, relatively little time is required to make a precision determination.

In each of these cases the proper type of source and crystal will also depend upon whether or not the background, due to the source in the neighborhood of the line, is large compared to the height of the line. This might be the case if the line in question were comparatively weak compared to other nearby lines in the same spectrum. It would also be true if the line were of such high energy that radiation penetrating the collimator contributed strongly to the background.

In case 1, the source and crystal used should be ones that maximize the quantity P. By using a 2 mm thick crystal instead of a 1 mm thick crystal, the reflected intensity at the peak of the line is doubled; that is to say, the quantity H appearing in formula 4 is doubled. On the other hand, the width of the line W is also doubled and therefore the factor $\frac{H}{W^2} \log \frac{H+B}{B}$ in the formula for P is never increased. It does, however, remain nearly constant if $B >> H$. If $B << H$, it decreases to little more than $\frac{1}{2}$ what is obtained with a thin crystal.

In case 2, one tries to obtain as many counts as possible from crystal reflection compared to statistical error of counting, to obtain the maximum probability of observing weak lines. This means that the area under the line profile should be maximized compared to the statistical error resulting from the background. A measure of the area under the line profile is given by HW, and the statistical error from background is $B^{\frac{1}{2}}$, so that $HW/B^{\frac{1}{2}}$ should be maximized. Since B is only increased very slightly when thicker crystals are used, while H and W seem to be about proportional to crystal thickness in the 1 to 2 mm range of thicknesses, considerable benefit is obtained by using thicker crystals, when case 2 obtains.

The situation concerning source <u>shape</u> is considerably more complex. Some radioisotopes may be chemically separable from their parent material and can, therefore, be condensed to a very small volume. This is true in general of fission products, naturally occuring radioactive materials and, in some cases, cyclotron activated sources. When this separation is possible, the source volume should

be made as small as possible with particular attention paid to narrowness of the source in order to obtain a sharp line. If the source width is made less than 0.001", it will not contribute appreciably to the width of the profile.

The majority of sources available in sufficient total activity for study with the spectrometer are of the neutron irradiated type. The radioactive material in nearly all such cases has the same atomic number as the parent, since it is produced by neutron capture. Chemical separation is, therefore, impossible and one finds that useful source intensity is determined by the maximum specific activity (activity per unit volume) available, rather than by total activity. Subsequent discussion of source shape will be concerned only with this type of source. Ideally, the active material should be concentrated within the focal volume so as to allow all parts of the source to make as nearly the same angle with the crystal as possible. Actually, this goal can be achieved fairly well by making the source rectangular with its depth about (dimension measured in the direction of propagation of the radiation from source to crystal) 40 times its thickness. Common dimensions for thickness and depth are 0.004" and 0.16". Its height is generally limited to about 1.25" to make the requirement that the source be parallel to the crystal planes less strict.

Certain advantages may be achieved by increasing the thickness of the source, keeping the depth and height at the above mentioned values. When this is done, the source profile alone assumes the shape of a broad rectangle. Upon folding this rectangle into the narrower

crystal window, one obtains a line profile having roughly the shape of a trapezoid with sides as steep as those of the usual triangular profile obtained with a narrow source. The height of this trapezoid will be the same as that of the triangle.

If (as in case 2 above) high precision is not desired, but one is merely trying to locate a line, this wide profile is more likely to be detected because, during the search, more time will be spent at positions of increased counting rate. Background due to the source will, of course, be increased and the advantage of a thicker source may be somewhat counteracted, since the total activity is increased in proportion to the thickness.

Curiously enough, the use of a thick source does not generally decrease the accuracy of a precision measurement. When running across a broad line profile there is no need to examine a high concentration of points on the flat top of the trapezoid, since in this region, the slope of the profile $L'(\lambda)$ is nearly zero. In formula 1 then, only those terms appear which are obtained from the sides of the trapezoid. Since the center section is mostly omitted, the entire analysis reduces to that of a triangular profile having the same height as the trapezoid, and formula 4 is still valid. Lower precision in this case is therefore only a result of higher background and not dependent directly upon the breadth of the profile.

Instead of using the radioactive sample itself to define line position, a slit composed of material having high gamma absorption may be placed at the crystal focus with a more extended source behind it. The theory of slit definition is discussed in D.J. Klein's thesis[12].

An illustration of the shape of such a slit is given in Fig. 22. Optimum results are obtained when the slit jaws form the angle subtended by the crystal at the source, since, in this way, penetration of the edges of the jaws by gamma rays from the source is minimized.

By use of the slit method, a much higher source profile can sometimes be obtained than by the source definition method, because any depth of radioactive material can be placed behind the source without causing front to back defocusing. Height of the line profile is then determined solely by radiation depth in the source material, if an unlimited amount of such material is available. On the other hand, a sharp rectangular profile, characteristic of the source definition method, is lost in this way because of penetration through the edges of the slit jaws. Clearly, advantages and disadvantages of this method must be weighed for each type of source material independently.

In the study of annihilation radiation[17], use of a slit is desirable because the relatively long range of the positrons make it impossible to confine annihilation to a narrow strip of material.

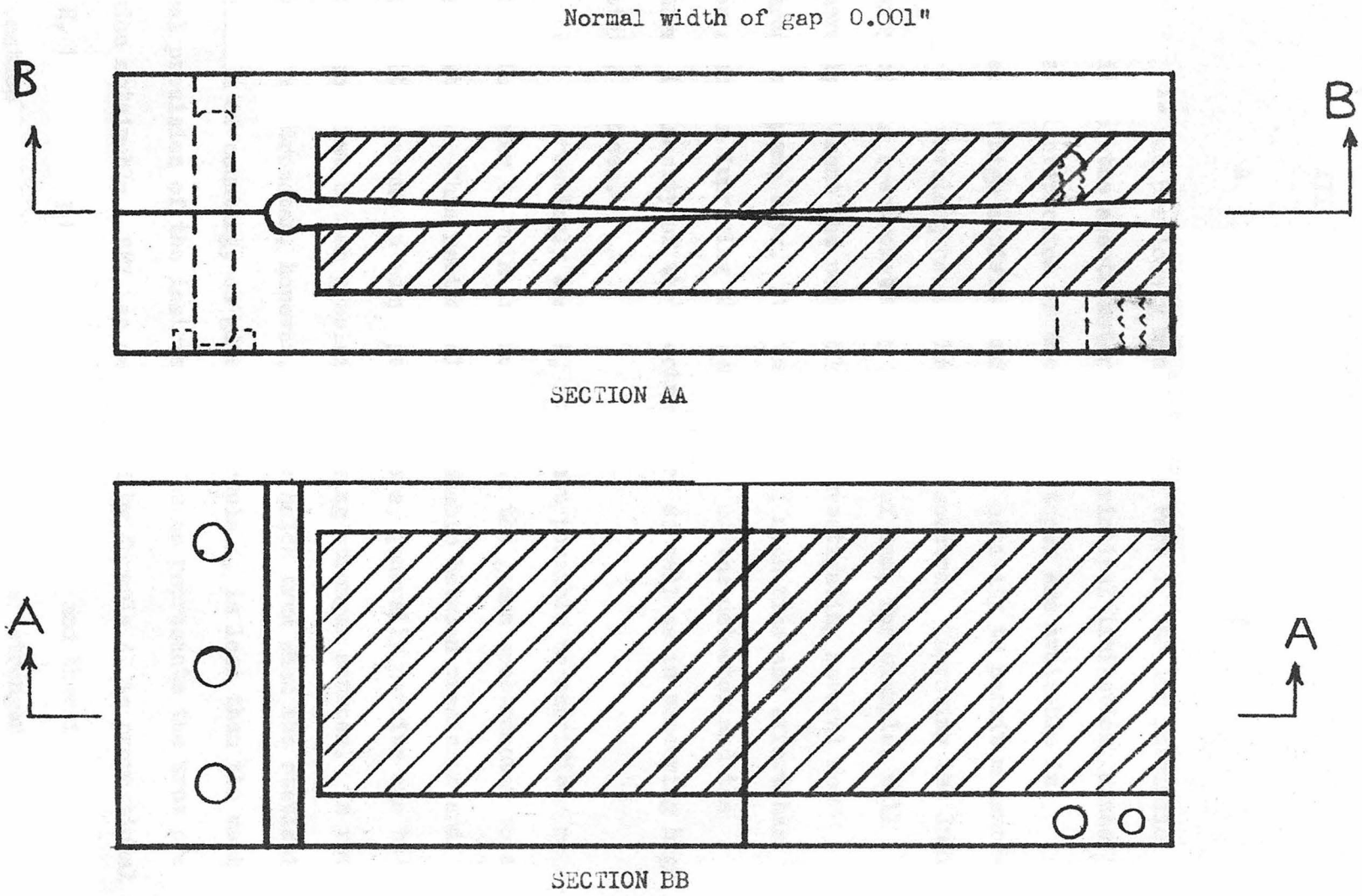

Fig. 22. Slit jaws for radiothorium source

III. CENTRAL PROBLEM OF LUMINOSITY

A. Advantages of High Luminosity

As was previously mentioned in Part I, the low intrinsic luminosity of the spectrometer is its principal limitation, since only a small proportion of the radioisotopes are available in sufficiently high activity and specific activity to permit measurement of the wavelengths of their gamma spectra. Improving the luminosity of the spectrometer by a factor of two, for example, will generally present the possibility of investigating several new sources of gamma rays. For this reason, much time and effort has been spent in improving the sensitivity of the detector and the general luminosity of the spectrometer, as well as in procuring high activity sources.

Interestingly enough, it is not possible to sacrifice resolution in order to gain luminosity with the gamma spectrometer to any great extent. This reciprocal relationship between precision and luminosity present in many spectrometers, generally permits one to obtain somewhat better precision by using stronger sources. In the crystal spectrometer, however, it only holds true when the statistical precision of counting, as given by formula 4, is less than the mechanical precision of the instrument and hence represents the true precision obtainable. "P", as determined by formula 4, is proportional to H, the counting rate at the peak of a line, and therefore one would automatically obtain greater precision by use of stronger sources. Even for relatively weak lines, however, the statistical precision of

counting is much better than the mechanical precision of the instrument, as may be seen from Table I. If a line is so weak that the error in determination of its position is mainly due to counting statistics, assumption 3, used in the development of formula 4, is no longer completely valid and the mere detection of the line becomes a problem. Therefore, we see that by using stronger sources, it is not possible to increase the precision of measurement, unless the line is so weak that it tends to fade into the background.

An important exception to the situation described above occurs when sources of sufficient strength are used to permit the obtaining of lines in second and third order reflections from the crystal. These reflections have intensities 0.013 and 0.005 times those obtained in the first order respectively. They occur at screw positions corresponding to two and three times the wavelength as measured in the first order, and since the error in screw divisions is taken as approximately constant, one obtains only $\frac{1}{2}$ and 1/3 the error in the second and third order determinations respectively that one obtains by the first order measurement. Of course, larger errors will be obtained if these other orders are so weak that accuracy is lost because of poor statistics of counting but, as we have seen, this will not generally be the case.

B. Intensity Calculations

Before undertaking the study of a gamma spectrum with the crystal spectrometer, it is extremely important to obtain some estimate of the strengths of the various lines in terms of counting rates obtain-

able with the detector. Sources may thus be classified according to their suitability for use in the spectrometer, and one may decide in advance which lines from these sources are worth-while attempting to locate.

Although the intrinsic luminosity of the instrument has already been discussed in various connections, a complete discussion has not been attempted. Intrinsic luminosity, we shall define as that fraction of the gamma rays of a particular energy emitted from the most favorable position in the source, which are counted by the detector, when the spectrometer is set at the position corresponding to this energy. Factors affecting the intrinsic luminosity will be discussed in order.

Solid angle subtended by the crystal. At a distance of two meters from the source, the crystal has a useful aperture consisting essentially of a rectangle of dimensions 1.7" x 2.0" and therefore subtending a solid angle of 5.5×10^{-4} steradians. It is doubtful that any improvement can be effected by moving the source closer to the crystal since then the crystal would have to be bent to a shorter radius of curvature and, in order to prevent breaking the crystal, a thinner sheet would have to be used. Furthermore, aberrations caused by the height of the crystal would be increased unless this height were reduced correspondingly, and a smaller volume of radioactive material could be placed near the focus.

Although the crystal aperture itself could probably be increased in size slightly, the difficulty of focusing would be increased proportionately and a larger collimator and detector would have to be

constructed to make use of the advantage.

Crystal reflectivity. As mentioned earlier, the fraction of incident gamma rays reflected from the crystal at the peak of a line, varies as the square of the wavelength. A comprehensive study of the reflection properties of a stressed crystal has been made by Lind[3,4] showing that this fraction is of the order of 10^{-3} for 2 mm crystals in the medium energy range. Besides the disadvantages mentioned in the section on precision, the use of crystals thicker than 2 mm is not feasible because of the increased possibility of breakage. Even several of the 2 mm crystals have broken after being bent to the 2 meter radius.

Collimator transmission. The collimator in use at present was designed ideally to have a transmission of 50%, since its tapered lead plates had exactly the same thickness as the spacers separating them. When its transmission was measured, however, it was found to lie between 30% and 40%, no doubt because of slight irregularities in the plates which tended to obscure some portions of the slots. Improvements in collimator design have been seriously considered, but the attendant difficulties have offset slight increases in luminosity to be gained. In particular, a collimator using tungsten instead of lead plates, so as to increase gamma absorption, was designed but the best tungsten plates obtainable proved to be too irregular for use in a collimator.

Detector efficiency. Detector efficiency may be taken as better than 50% in the range of energies 0.05 to 1.0 Mev. At the high energy end, the efficiency falls off because of reduced absorption by the Na(Tl) crystal, while at the low end it is reduced because the small scintillations blend with the noise.

If one multiplies the four factors mentioned above, the result 7.5×10^{-9}, represents an order of magnitude estimate of the intrinsic

luminosity. A 10 millicurie gamma ray source with ideal geometrical features could therefore only produce $(3.7 \times 10^{8}) \times (7.5 \times 10^{-9}) = 2.8$ counts per second in the detector at the peak of its line, whereas the irreducible background amounts to about 5 counts per second.

Absorption in the Source. Apart from considerations of source activity and specific activity, discussed in Part II, absorption of gamma radiation by the source material itself reduces the apparent activity of the source in the case of soft, highly absorbed gamma radiation.

If the mean absorption distance in the source material for a particular energy of radiation is L, and the depth of the source is D, then by simple calculation, it can be shown that the intensity is reduced by a factor of $\frac{1-e^{-D/L}}{D/L}$ because of absorption in the source. As would be expected, this factor approaches 1 when L approaches infinity, and strangely enough, when D/L becomes large, the source emits as if its depth were only L. Between these two extremes the effective depth of the source remains less than the smaller of the two quantities L (the mean absorption depth) and D (the true depth). The fact that the effective depth can never be greater than L, means that in many cases the advantage gained by increased crystal reflection at long wavelengths is more than offset by absorption in the source itself, which increases at a much more rapid rate.

Absorption in the quartz crystal, and in the window of the scintillation counter, also has a slight effect at very long wavelengths; but for the most part this absorption can be ignored.

Half-life. While the various factors mentioned above must be weighed together when evaluating the suitability of a particular radioisotope for study, one must also take into consideration the half-life

of the material, whenever it is short enough to limit the time spent in the investigation. If extremely short-lived sources are used, the time spent in transporting the material from its place of manufacture will often amount to several half-lives.

The shortest lived source to have been successfully investigated with the gamma-ray spectrometer was copper 64, used in the study of annihilation radiation, with a half-life of 12 hours. Other short-lived sources studied with the spectrometer have been, rhenium 188 (half-life 18 hrs.), tungsten 187 (half-life 24 hrs.), gold 198 (half-life 2.7 days), radon (half-life 3.8 days), and iodine 131 (half-life 8 days). A practical limit on the minimum half-life of source materials is probably about 6 hours, since this represents about the shortest feasible interval for a run on a line.*

The following is a summary of the various factors affecting line strength.

1. Solid angle subtended by the crystal. } Intrinsic Luminosity
2. Crystal reflectivity
3. Collimator transmission.
4. Detector efficiency.
5. Absorption by the source. } Source Features
6. Half-life. (Indirectly)

Naturally, one must also bear in mind that certain gamma rays do not occur with every disintegration of a nucleus and for

---

* However, construction of a spectrometer capable of operating with sources which are continuously activated while they are being analyzed spectrally is contemplated.

this reason, the activity of a source measured in disintegrations per second will misrepresent the gamma activity. Reasons for reduced gamma activity may be listed as follows:

Complex beta decay. If a certain amount of beta decay takes place to the ground state of the daughter nucleus as well as to an excited state, the gamma activity will only correspond to that fraction of the decay resulting in an excited nucleus.

Branching of gamma decay schemes. Whenever an excited level of the daughter nucleus can decay by two or more types of gamma cascades, the individual gamma rays involved will not occur with every disintegration of the nucleus, but only when the cascade in which they lie occurs.

Internal conversion. Internal conversion will rob the nucleus of the possibility of emitting a gamma ray with the result that large internal conversion coefficients will mean lowered gamma activity.

To illustrate how intensities are estimated, a sample calculation is provided here of the intensity to be expected of the 618 kev. line of tungsten 187. This line, which has proved rather difficult to measure, represents a case of marginal practicality. Intrinsic luminosity features may be listed as follows:

1. Fraction of emitted radiation striking crystal - 4.5×10^{-5}
2. Crystal reflectivity at 618 kev. - 7.3×10^{-4}
3. Collimator transmission - 1/3
4. Detector efficiency - 0.7

618 kev. radiation has a mean absorption depth in metallic tungsten of 0.53 cm. and if a strip of depth 0.63 cm. is used, the fraction of the

radiation escaping will be 0.58. By multiplying these five factors together we obtain the fraction F of the emitted radiation which is counted in the detector.

$$F = 4.5 \times 7.3 \times 0.33 \times 0.7 \times 0.58 \times 10^{-9} = 4.5 \times 10^{-9}$$

In the Oak Ridge catalogue, the activity available in tungsten 187 is listed as 350 millicuries per gram, but since this figure is given for WO_3 we may expect an activity of 420 millicuries in a gram of pure tungsten. This activity, present when the sample is removed from the pile, will have decayed to $\frac{1}{2}$ this value after the 24 hours required for air freight transportation to Pasadena. We may expect, therefore, an activity of

$$\frac{1}{2} \times 420 \times 3.7 \times 10^{7} = 7.8 \times 10^{9} \text{ disintegrations per second}$$

at the time of arrival of the sample. Unfortunately, not all disintegrations give rise to gamma radiation, because 30% of the beta rays emitted by tungsten 187 leave the resulting rhenium nucleus in its ground state. The remaining 70% give rise to gamma radiation, but of these only 10% are followed by the 618 kev. line. We obtain, therefore, $7.8 \times 10^{9} \times 0.7 \times 0.1 = 5.5 \times 10^{8}$ gamma rays per second of 618 kev. from the one gram source. In terms of detector counts, we may expect $5.5 \times 10^{8} \times 4.5 \times 10^{-9} = 2.5$ counts per second. This line is, therefore, a fairly weak one since the irreducible background counting rate amounts to about 5 counts per second.

C. Procurement of Radioactive Materials

By far the greatest number of radioisotopes investigated with the gamma ray spectrometer so far, have been those neutron-rich isotopes which can be formed by capture of thermal neutrons in a pile. Samples of material having large thermal neutron crossection can be activated to high specific activity in this way. Radioisotopes of this type, with high atomic number, often emit gamma rays following beta decay to an excited state of a stable nucleus.

Isotopes formed in this way are limited to a specific activity proportional to the neutron flux in the pile, but are only limited in total activity by the size of the sample being irradiated. It is necessary, therefore, to be concerned with problems of source shape and absorption in the source, when preparing samples for neutron irradiation because of the presence of relatively large amounts of inseparable inactive material in the activated source. Improvements in source activity can be produced by allowing a sample to remain in the pile for long periods of time, however, no advantage is achieved by leaving it for more than 3 or 4 half-lives, since by that time the rate of decay of the isotope is almost in equilibrium with its rate of formation.

Other radioisotopes occuring as fission products or as naturally radioactive materials can sometimes be obtained in sufficient strength to permit study. It is also quite likely that cyclotron activated materials could be used now that increases have been made in luminosity of the spectrometer.

IV. DESCRIPTION OF RESULTS

A. Preparation of a Source of Iridium 192 and its Investigation with the Curved Crystal Spectrometer

Iridium 192 was chosen for study with the spectrometer because it was known to emit a multitude of different gamma rays whose energies were only approximately known. In addition to being an interesting source for study, it was possible by neutron irradiation in a pile, to prepare a sample of extremely high specific activity, because of its large yield in the neutron capture of iridium 191. This last feature, combined with its long half-life of 70 days, made its study most advantageous.

The iridium sample was prepared for irradiation by packing .560 grams of iridium powder into a suitably shaped container made of pure aluminum. Aluminum was used for this container since it does not become appreciably radioactive when subjected to neutron bombardment. This container was fabricated from a piece of $\frac{1}{4}$" aluminum tubing, which was compressed between specially constructed vise jaws so that the hole passing through the tubing assumed dimensions suitable for a source. In the case of iridium, the source chamber had the dimensions 1.25" x 0.215" x 0.010". The narrow edge was placed so as to face the crystal, and in order to allow soft radiation to pass from the source, the aluminum covering was milled away from this edge. Uncovered edges of the sample were then sealed with Glyptal to prevent bits of radioactive iridium from falling out of the aluminum chamber.

Arrangements were made for irradiation of the sample at the

Argonne National Laboratory, where a pile having three times the neutron flux of the one at Oak Ridge is available. An even higher neutron flux is available at the pile in Chalk River, Ontario, but at the time of the irradiation of this sample, international regulations prevented our use of these facilities. The actual irradiation lasted the four months from the end of September 1950, to the end of January 1951. At the end of this time, the source was so intensely radioactive that it was necessary to allow it to decay for two weeks, to eliminate the 19 hour activity of iridium 194, before shipment was permissible. At the time of shipment, the activity of the sample was estimated by the Argonne National Laboratory as being 2.7 curies, but our measurements indicate that it was somewhat higher.

After placing the source in the spectrometer, a complete search was made for gamma rays and x-rays having wavelengths from zero to 400 milliangstroms. For this purpose, a Brown Recorder was attached to a counting rate meter so as to register the counting rate while the spectrometer's precision screw was turned continuously by means of the small setting motor over the range of positions under investigation. In this way, most of the lines which were intense enough to study were detected in about four hours of running time. Later, a more intensive search over the region from zero to 200 milliangstroms was made using the standard robot operation moving the screw in discrete steps at a rate of 0.1 milliangstrom per minute. This search revealed a few additional lines which were too weak to be picked up with the counting rate meter. In all, 38 separate peaks were revealed during the search, corresponding to gamma rays obtained in first, second, and third orders,

and K x-rays from osmium, iridium, and platinum. Precision measurements of these peaks were then made in the usual manner by totaling counts every 21 minutes at points on the line profile spaced .04 screw divisions apart. In this way, a single peak could be covered easily in 12 hours and a pair of line profiles corresponding to a gamma ray energy could be run in 24 hours. In spite of 24 hour a day operation, the complete study of the gamma and x-ray spectra from this source took nearly two months.

B. Decay of Iridium 192

Iridium 192 has been found to decay with a half life of 70 days by β^- emission to platinum 192. The end point of the β^- spectrum, as measured by Mandeville and Scherb and others[18,19,20] corresponds to an energy of about 0.6 Mev., the exact end point being difficult to measure because it is obscured by conversion lines. A simple spectrum is thought to exist, however, since the ratio of beta-gamma coincidence counting rate to beta counting rate does not seem to vary as beta absorber is placed in front of the beta counter. Mandeville and Scherb have also found by means of coincidence measurements that each beta ray is followed on the average by 0.6 Mev. of gamma radiation.

One may infer from the presence of osmium K x-rays among those from iridium and platinum, that iridium 192 also decays by the process of K capture to osmium 192 with the possible emission of gamma rays following this decay. K capture leaves the atom of osmium ionized in the K shell, thus giving rise to K x-rays. In a recent paper, Cork

has confirmed this conclusion by detecting Auger electrons corresponding to osmium x-rays[21].

It is, of course, impossible to determine with the gamma ray spectrometer which of the measured gamma lines result from transitions in platinum and which from those in osmium. By establishment of definite decay schemes, however, one might be able to group certain gamma rays together which come from a single element. Very likely, a definite assignment could be made by beta-gamma coincidence techniques.

A list of measured x-ray lines is given in Table II, where present measurements of wavelengths are compared with those of Ingelstam[22]. Intensities of the K spectra of osmium, iridium, and platinum were observed to lie in the ratio 1 : 1.7 : 1.3. While K lines of iridium are, no doubt, excited by flourescent absorption of gamma rays in the source material, those of platinum must be produced by internal conversion of the gamma rays following β^- decay. Since internal conversion does not necessarily follow β^- decay, it is not possible to determine quantitatively, from a comparison of x-ray intensities, the relative probabilities of K capture and β^- decay. On the other hand, we can be certain that the latter has the greater probability, since osmium x-rays are the least intense of all.

C. Gamma Radiation Following the Decay of Iridium 192

By studying characteristics of the peaks obtained during the search for lines from iridium 192, it is possible to make an interpretation of them in terms of gamma rays and x-rays appearing in the first, second and third orders of reflection from the quartz crystal.

Table II

Wavelengths in Milliangstroms of X-Ray

Lines Emitted by the Source of Iridium 192

Designation	Present Measurement	Measurement by Ingelstam
Os $K\alpha_2$	201.622	201.627
Os $K\alpha_2$	196.774	196.783
Ir $K\alpha_2$	195.868	195.889
Ir $K\alpha_1$	191.025	191.033
Pt $K\alpha_2$	190.366	190.372
Pt $K\alpha_1$	185.493	185.504
Os $K\beta_3$	174.088	174.072
Os $K\beta_1$	173.581	173.607
Ir $K\beta_3$	169.349	169.357
Ir $K\beta_1$	168.528	168.533
*	165.567	
*	165.136	
Pt $K\beta_3$	164.469	164.489
Ir $K\beta_2^{II}$	164.013	164.139
Ir $K\beta_2^{I}$		163.944
Pt $K\beta_1$	163.670	163.664
Pt $K\beta_2^{II}$	159.257	159.374
Pt $K\beta_2^{I}$		159.184

* The two weak lines at 165.567 milliangstroms and 165.136 milliangstroms remain unidentified and may be gamma rays.

X-ray lines may be identified in a number of ways. In the first place, their wavelengths are fairly well known so that by accurate measurement alone a positive identification can be made. Secondly, the natural breadths of the K lines are quite comparable to the instrumental window of the spectrometer so that they appear detectably broader than gamma lines,whose natural breadth is quite negligible. Finally, the x-ray lines appear in characteristic series having definite intensity ratios, so that a complete series may be expected, and the positions of the lines predicted ahead of time.

Second and third orders of intense gamma and x-ray lines may be sought at spectrometer screw positions corresponding to two and three times the wavelength of the first order reflections. Intensities of first to second to third order reflections were found to lie in the ratio of 1 : 0.013 : 0.005. Identification of the various orders was thus achieved by comparing screw positions and intensities. Whenever any doubt existed, however, a positive identification was made by use of the scintillation counter as a low resolution spectrometer, operating in tandem with the crystal diffraction spectrometer, to separate orders of reflection. Gamma and x-ray lines will thus produce scintillation pulse height spectra corresponding to the energy of the reflected photons and independent of the order of reflection.

Using the above methods, it was possible to pick out from the 38 peaks originally noted, 13 distinct gamma rays lying between the energies of 84.1846 kev. and 612.44 kev. Of these thirteen, the two weakest ones, having energies in the neighborhood of 84.7 kev. and

87.3 kev., consist of a large number of closely spaced components. Seven different components were observed between the energies of 84.1846 kev. and 85.1977 kev. The weaker multiplet, lying between 87.1467 kev. and 87.4387 kev., could easily have as many components, but due to its low intensity, it was impossible to separate more than three.*

Four gamma rays, having energies of 467.53 kev., 316.28 kev., 308.26 kev., and 295.79 kev., were five to ten times as intense as any other lines present and were all obtained in the second and third orders as well as in the first order. Four much weaker lines of higher energy were also measured at energies of 484.48 kev., 588.04 kev., 604.17 kev., and 612.44 kev., the last pair comprising a fairly close doublet which had to be separated by use of the composite profile method. A complete list of gamma ray wavelengths and energies, together with their approximate intensities and estimated errors is given in Table III, while a comparison of these measurements with results previously obtained with beta-ray spectrometers is given in Table IV. For the sake of consistency, only first order measurements are listed in these tables.

A decay scheme involving all but the four gamma lines at 201.267 kev., 205.658 kev., 484.48 kev., and 588.04 kev. may be constructed, as shown in Fig. 23, in which different Ritz combinations of the various lines agree in energy to better than their estimated errors. This scheme is also in good agreement with observed intensities. As well as providing five major levels, arising from combinations of the lines at 136.294 kev., 295.79 kev., 308.26 kev., 316.28 kev.,

* See supplement concerning assignment of these apparent multiplets.

Table III

Wavelength and Quantum Energies of the Gamma Rays Following Decay of Iridium 192 as Measured in the First Order.

Wavelength in Milliangstroms	Energy in Kev.	Relative Intensity
20.241 ± .030	612.44 ± .91	50
20.587 ± .020	604.17 ± .59	137
21.081 ± .020	588.04 ± .55	106
25.587 ± .020	488.48 ± .38	116
26.515 ± .020	467.53 ± .35	3044
39.195 ± .020	316.28 ± .16	9896
40.214 ± .020	308.26 ± .15	3744
41.909 ± .020	295.79 ± .14	3840
60.277 ± .020	205.658 ± .068	753
61.592 ± .020	201.267 ± .065	106
90.954 ± .020	136.294 ± .030	42
141.773 ± .040	87.4387 ± .025	7
142.085 ± .040	87.2466 ± .025	
142.248 ± .040	87.1467 ± .025	
145.502 ± .040	85.1977 ± .023	14
145.769 ± .020	85.0417 ± .012	
146.155 ± .020	84.8171 ± .012	
146.390 ± .040	84.6809 ± .023	
146.599 ± .040	84.5602 ± .023	
146.985 ± .040	84.3381 ± .023	
147.253 ± .040	84.1846 ± .023	

It should be noted that for sake of consistency only those measurements from first order reflections are included in this table.

Table IV

A Comparison of Present Measurements With Various Other Determinations of Gamma Ray Energies From Iridium 192

Present Measurement	Ref. 23	Ref. 24	Ref. 25	Ref. 26
136.294	137			
201.267				
205.658	208	209	269	
295.79	296	295	294	
308.26	308	307	306	307
316.28	317	316	315	
467.53		468	466	467
484.48		488	477	
588.04		591	586	
604.17		607	601	603
612.44		615	610	
			651	

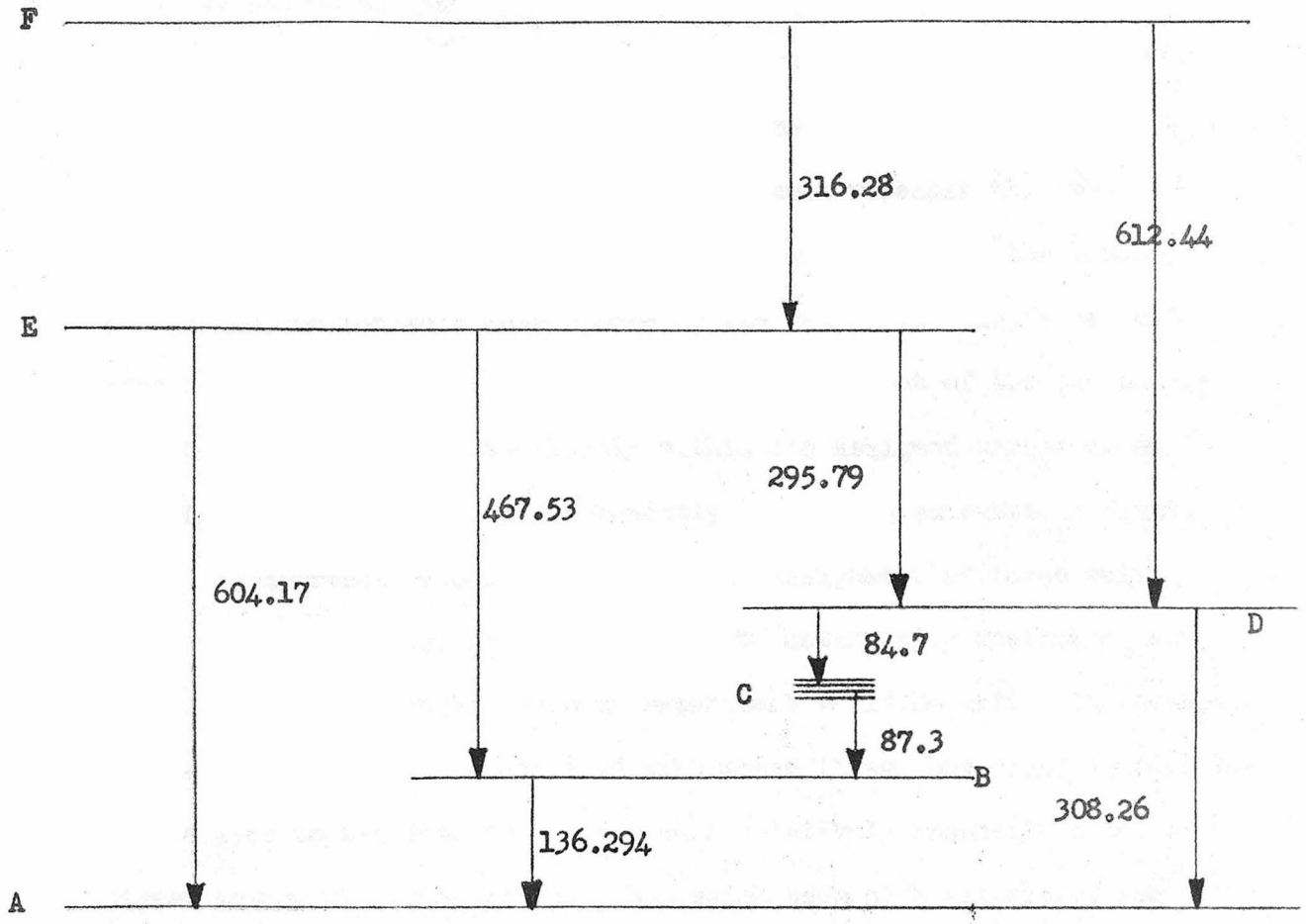

Fig. 23. Proposed decay scheme for the gamma rays from iridium 192.

467.53 kev., 604.17 kev., and 612.44 kev., one can include the two low energy multiplets at 84.7 kev., and 87.3 kev., if it is assumed that they are in cascade, and taken together represent a transition from the second excited level at 308.26 kev. to the first excited level at 136.294 kev. Although it is true that seven components were separated from the multiplet at 84.7 kev., while the one at 87.3 kev appeared to have only three, one must remember that the higher energy multiplet is only about half as intense as the lower energy one and for this reason some of its weaker components may not have been detectable. Nevertheless, this assignment of the low energy multiplets does not lie as closely within the assigned errors as do the other combinations and consequently it remains somewhat in doubt.

Important evidence regarding the assignment of these multiplets could be gleaned from an experiment determining whether or not they lie in coincidence. Such an experiment would be difficult because of the low intensities associated with these lines, but might be possible if one were to use detectors which were relatively insensitive to the higher energy radiation present, but which have high efficiency for gamma rays with energy in the neighborhood of 85 kev. X-ray counters or beta ray counters might be used in this application, or even thin crystal scintillation counters if large scintillations produced by the higher energy gamma rays are discriminated against electronically.

A small source of iridium 192 might be placed between two such counters operating in coincidence. Between the source and the counters, one might then insert, alternately, filters of gold and lead whose thickness would be so adjusted that they had the same absorption for the

higher energy gammas and the x-rays,as in the Ross method of balanced filters. Since the energies of the multiplets lie between the K absorption limits of lead and gold, the absorption of these lines would be much greater in the gold, which can absorb this radiation by flourescent absorption in its K shell, than in lead which has too high an atomic number for this to occur. If these gamma rays are truly in coincidence, as is predicted by the decay scheme, one would expect to notice a higher coincidence counting rate when using the lead filter than when using the gold.

The following combinations of gamma ray energies permitted the construction of the decay scheme:

$$295.79 \text{ kev.} + 308.26 \text{ kev.} \doteq 604.17 \text{ kev.}$$

$$136.294 \text{ kev.} + 467.53 \text{ kev.} \doteq 604.17 \text{ kev.}$$

$$295.79 \text{ kev.} + 316.28 \text{ kev.} \doteq 612.44 \text{ kev.}$$

$$84.7 \text{ kev.} + 87.3 \text{ kev.} + 136.294 \text{ kev.} \doteq 308.26 \text{ kev.}$$

Gamma ray energies combine with such exactness that the validity of these combinations seems practically certain. The decay scheme of Fig. 23, which was divined from these combinations is, however, by no means unique, since by permuting the orders of the various lines within the combinations, it is possible to arrive at other decay schemes. Decay schemes obtained in this way such as the one in Fig. 24 involve the same combinations, but are otherwise quite different. This decay scheme has the advantage over the first decay scheme of agreeing with the assertion of Mandeville and Scherb that 0.6 Mev. of gamma radiation follow beta emission, but the disadvantage not present in the first scheme of disagreeing decidely with the

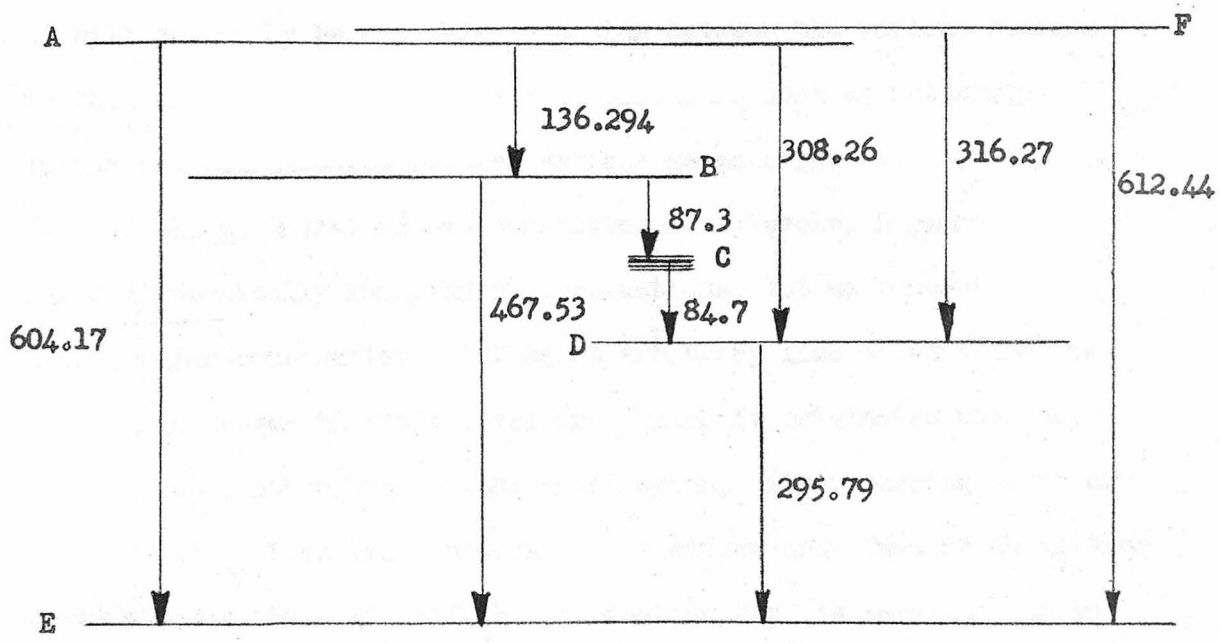

Fig. 24. Alternate decay scheme for the gamma rays from iridium 192.

intensity ratios noted during the present measurements*.

Since various decay schemes may be constructed from a given set of combinations, it is of interest to see how many ways a given set of combinations may be permuted to give different schemes, and to attempt to devise a system for discovering these schemes quickly and easily. Once this purely mathematical question has been answered, it will generally be possible to decide between the various schemes on the basis of other physical considerations such as intensity ratios and coincidences between various gamma rays.

In a general scheme consisting of N levels, L gamma lines, and C algebraically independent combinations, let us concentrate on a particular combination. Taking an arbitrary line of this combination, we discover that the level from which it originates has one, and only one, other line of the combination, either passing to it or away from it. This line in turn passes either away from or to another level where a third line of the combination has its terminus, so we may pass in a circuit around the various lines of the combination until we arrive at the original line where we started. Such a circuit may be represented graphically as a loop with the various levels appearing as dots or points and the gamma lines as the connecting lines between these points. Other combinations involving perhaps

---

* Intensities of the lines at 295.79 kev. and 308.26 kev are about the same, while the intensity of the one at 316.27 kev. is more than twice this. In the scheme of Fig. 24, one would expect the intensity of the 295.79 kev. line to be greater than the sum of the other two.

some of the same gamma rays, form other circuits containing points (or levels) and lines in common with this one and the whole is thus represented as a network. In this network, the lengths of the various lines in no way correspond to gamma ray energies, and consequently this representation conveys no numerical information concerning the combinations, but instead may be used to show at a glance their topology. The network representation of the iridium decay scheme is shown in the upper drawing of Fig. 25.

Given such a network, it is possible to construct the associated decay scheme if one knows the line energies and the signs to be attached to these energies in each circuit. (A positive sign may be arbitrarily attached to a line in a combination if, as one passes around a circuit, one goes from the final to the initial state, while a negative sign may be attached if one goes from the initial to the final. The algebraic sums of the lines contained in any circuit is therefore zero).

Once the network representation for a decay scheme has been obtained, it is possible to arrive at other decay schemes having the same independent combinations (or circuits) by permuting the orders of lines appearing in the various circuits in such a way as to avoid changing the lines appearing in any circuit. In the lower drawing of Fig. 25, lines a and b have been interchanged, thus changing the decay scheme from the one appearing in Fig. 23, represented by the upper drawing of Fig. 25, to the one appearing in Fig. 24. Clearly, still other decay schemes could be constructed by interchanging c and d, or by interchanging both c and d, and a and b. Still more schemes may be

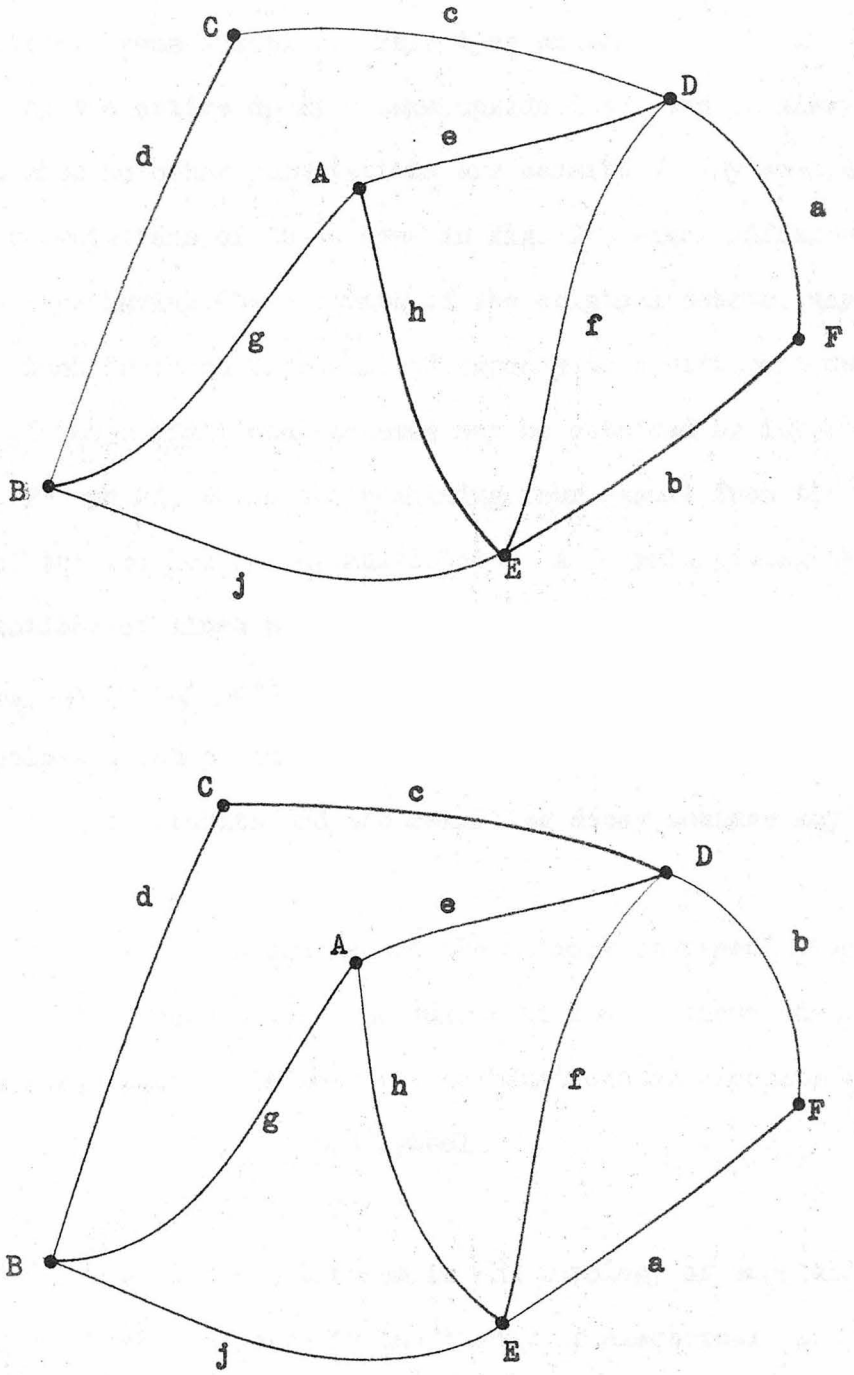

Fig. 25. Topological representation of the decay schemes of figures 23 (above) and 24 (below).

constructed by inverting the orders of all lines in all the circuits thus effecting a mirror transformation. This type of transformation corresponds to turning the entire decay scheme upside down, and is always possible even when no other permutations are permitted. By considering all possible permutations of the scheme in Fig. 23, eight different networks of this type having the circuits of the original scheme, may be constructed. Each of these networks corresponds to a different decay scheme. Two of these additional schemes may be obtained by inverting those of Fig. 23 and 24, while the remaining four result from the trivial interchange of the two low energy multiplets. A formula giving the number of permutations of lines possible with a general network has not been obtained here, but in any particular case, a quick inspection of the network will disclose which permutations of lines may be made without destroying the existing circuits and the resulting decay schemes may be constructed.

An interesting consequence of the network representation of decay schemes is the theorem that the number of levels minus the number of lines plus the number of independent combinations or circuits equals 1. Or using the previously defined symbols

$$N - L + C = 1$$

This theorem, known as Euler's theorem in the topology of maps and networks, and which also appears in the theory of electrical circuits[27], enables one to predict the number of levels obtainable with a certain number of lines and independent combinations, before a decay scheme has even been constructed.

D. Precision of Measurements

Many checks on the precision of the spectrometer were made possible by the study of the spectrum of iridium 192. The following methods were used to estimate non-linearities and non-reproducibilities.

1. Repetition of the measurement of the 316.28 kev. line at regular intervals during the study of the other lines of the spectrum, gave a check on the reproducibility of the spectrometer. In all, five measurements of the line were made with the following results.

No. of Run	Wavelength in Milliangstroms
1	39.195
2	39.199
3	39.210
4	39.189
5	39.191
Average	39.197

This particular group of measurements has a root mean square deviation from the mean of 0.007 milliangstroms*. Former repetitions of runs, using other radioactive sources, have yielded similar deviations, and while variations as large as 0.010 milliangstroms are unlikely, the fact that they do occur occasionally makes a choice of this figure for the non-reproducibility seem reasonable. (See Table I).

2. Second and third order reflections of the intense lines

---

* The figure 0.007 milliangstroms was obtained by taking the square root of the average square of the deviations from the mean.

of the iridium have provided an excellent check on the linearity of the entire instrument over most of the gamma ray range. Wavelengths of the four intense gamma lines as measured in the first, second, and third orders are given in milliangstroms.

Energy	3rd Order	2nd Order	1st Order
295.79 kev.	41.898	41.894	41.909
308.26 kev.	40.191	40.205	40.214
316.28 kev.	39.174	39.183	39.197
467.53 kev.	26.496	26.503	26.515

In all cases except one, higher order wavelength measurements are smaller, the difference between measurements in successive orders being on the average about 0.01 milliangstroms. Non-linearities in the range from 125 milliangstroms to 26 milliangstroms definitely seem to be indicated by these results. These deviations, which can be as great as 0.02 milliangstroms, are of sufficient magnitude and correct sign to account for the difference between the wavelength of annihilation radiation, 24.271 milliangstroms, as measured by the crystal spectrometer, and the Compton wavelength of the electron, 24.26067 milliangstroms[28]. The anomalous results of Lind and Hedgran[29], which are principally based upon the crystal measurement of the 411 kev. line of gold 198, can be explained in the same way.

A second order reflection of the intense $K\alpha_1$ line of iridium was also obtained, thus permitting a linearity check on the instrument over almost its entire scale. In the second order, its wavelength measured 190.993 milliangstroms, while the first order measurements

produced the result 191.025 milliangstroms, thus confirming the trend observed within the shorter region.

3. Additional checks on the linearity of the spectrometer were possible by means of the various Ritz combinations which were noted in the iridium spectrum and which are listed on page 108. These combinations all hold true well within the errors which were assigned on the basis of the linearity and reproducibility checks.

4. In the long wavelength region from 200 milliangstroms to 160 milliangstroms, the x-ray K spectra of osmium, iridium, and platinum presented in Table II may be used as a direct check on the absolute calibration of the spectrometer. For the most part, the present measurements of the major x-ray lines agree well with the results of Ingelstam, although his wavelength measurements tend to be a trifle lower.

An absolute calibration of the spectrometer was made two weeks after the investigation of the iridium spectrum. This calibration, which has always been made in the past by running the tungsten $K\alpha_1$ line using an x-ray tube placed behind a slit, was made for the first time by use of a source of tantalum 182. Excitation of the tungsten $K\alpha_1$ line occurs in this source by internal conversion of one of the gamma rays emitted by the excited tungsten 182, resulting from the beta decay of tantalum 182. In this way, it was possible to make a calibration under exactly the same conditions that exist during the investigation of gamma ray lines; conditions which could never be simulated exactly because of the change in load on the spectrometer when the x-ray tube was placed on its carriage and because

of the pull of the cables upon the tube, which might tend to displace the slit somewhat. The result of this calibration, however, agreed well with the most recent calibration by the x-ray tube method; the screw factor being 1.00184 milliangstroms per revolution of the spectrometer precision screw.

E. Study of the Gamma Ray Spectrum of Tungsten 187

A one gram strip of tungsten, irradiated in the pile at the Oak Ridge National Laboratory, was used for the study of the gamma ray spectrum following the decay of tungsten 187. Since tungsten 187 is β^- active with only a 24 hour half life, it was necessary to fly the irradiated source by air freight to Pasadena so as to minimize the loss of activity during the time spent enroute. In spite of attempts to speed transportation as much as possible, four separate irradiations were required before measurements of the five gamma ray lines could be completed.

Results of the measurements of the five known gamma rays of tungsten 187 are in essential agreement with previous measurements[30,31,32]

Table V

Wavelengths and Quantum Energies of Tungsten 187 Gamma Ray Lines

Wavelength in Milliangstroms	Energy in kev.
18.077 ± .020	685.76 ± .74
20.043 ± .020	618.49 ± .62
25.866 ± .020	479.26 ± .38
92.359 ± .020	134.220 ± .028
172.153 ± .020	72.008 ± .008

The decay scheme of Beach, Peacock, and Wilkinson[30,31] appears to be correct in so far as the combination 72.008 kev. + 134.220 kev. + 479.26 kev. ≐ 685.76 kev. checks well within instrumental errors, but the line at 618.492 kev. does not combine with the 134.220 kev. and 479.256 kev. lines, as indicated in their decay scheme. The corrected decay scheme for tungsten 187 shown in Fig. 26 does not include the 618.492 kev. line, which apparently represents an independent transition.

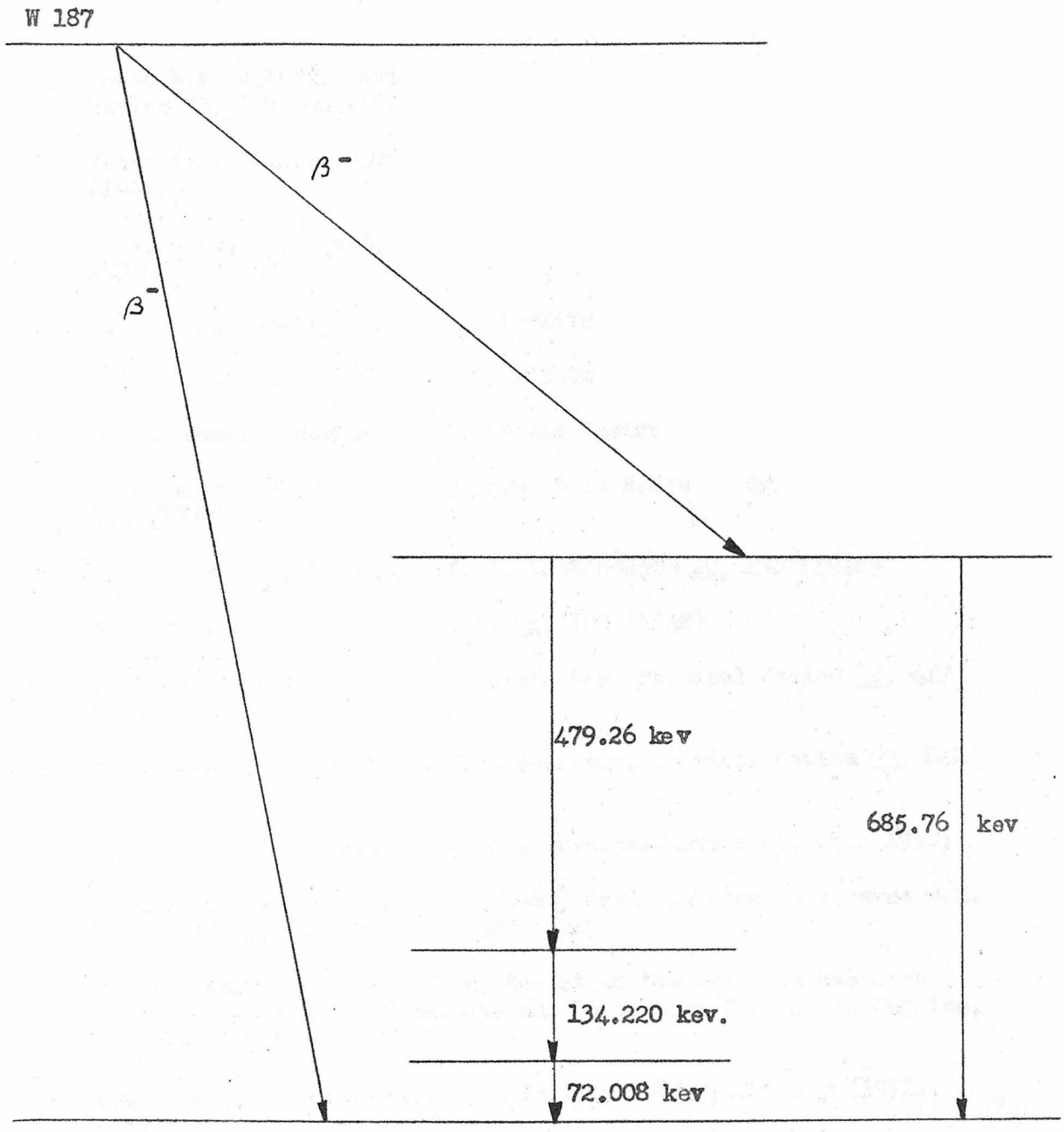

Fig. 26. Corrected decay scheme for W 187.

Bibliography

1. Jesse W.M. DuMond, David A. Lind, and Bernard B. Watson, Physical Review 73, 1392-94 (1948)

2. Jesse W.M. DuMond, Review of Scientific Instruments 18, 626-638 (1947)

3. D. A. Lind, W.J. West, and J.W.M. DuMond, Physical Review 77, 475-490 (1950)

4. D.A. Lind, Thesis, California Institute of Technology (1948)

5. J.R. Brown, Thesis, California Institute of Technology (1951)

6. J.W.M. DuMond, Review of Scientific Instruments 1, 2 (1930)

7. Y. Cauchois, Journal de Physique et le Radium, Series 7, No. 3, 320 (1932)

8. D.A. Lind, Review of Scientific Instruments 20, 233 (1948)

9. R. Hofstadter, Physical Review 74, 100 (1948)

10. John A. McIntyre and Robert Hofstadter, Physical Review 78, 617 (1950)

11. R.W. Pringle, S. Standil, K.I. Roulstom, Physical Review 77, 841 (1950)

12. R. Hofstadter and J.A. McIntyre, Physical Review 80, 631 (1950)

13. Bernard B. Watson, William J. West, David A. Lind, and Jesse W.M. DuMond, Physical Review 75, 505 (1949)

14. J.W.M. DuMond and E.R. Cohen, Report to the National Research Council Committee on Constants and Conversion Factors of Physics, December (1950)

15. D.J. Klein, Thesis, California Institute of Technology (1951)

16. J.W.M. DuMond, D.A. Lind, and E.R. Cohen, Review of Scientific Instruments 18, 617 (1947)

17. J.W.M. DuMond, D.A. Lind, and B.B. Watson, Physical Review 75, 1226 (1949)

18. C.E. Mandeville, M.V. Scherb, Physical Review 73, 1434 (1948)

19. L.J. Goodman and M.L. Pool, Physical Review 71, 288 (1947)

20. P.W. Levy, Physical Review 72, 352 (1947)

21. J.M. Cork, J.M. Le Blanc, A.E. Stoddard, W.J. Childs, C.E. Branyan, and D.W. Martin, Bulletin of the American Physical Society 26, No. 3, 31 (1951)

22. E. Ingelstam, Nova Acta Reg. Soc. Sci. upsal. (4) No. 5 (1936)

23. R.D. Hill, W.E. Meyerhof, Physical Review 73, 812 (1948)

24. P.W. Levy, Physical Review 72, 352 (1947)

25. J.M. Cork, Physical Review 72, 581 (1947)

26. M. Deutsch, Physical Review 64, 265 (1943)

27. W.R. Smythe, Static and Dynamic Electricity, McGraw-Hill Book Co., 222 (1939)

28. J.W.M. DuMond, Physical Review 81, 468 (1951)

29. Arne Hedgran and David A. Lind, Physical Review 82, 126 (1951)

30. L.A. Beach, Charles L. Peacock, and Rodger O. Wilkinson, Physical Review 75, 211 (1949)

31. C.L. Peacock and R.G. Wilkinson, Physical Review 74, 601 (1948)

32. N. Hole, J. Benes, A. Hedgran, Arkiv. Mat. Astron. Fysik 35A, No. 35 (1948)

SUPPLEMENT

The author is greatly indebted to Professor R. P. Feynman for pointing out that the multiplets in the neighborhoods of 84.7 kev and 87.3 kev may be identified with the $K\beta_3$, $K\beta_1$ doublet and the $K\beta_2$ doublet respectively in the x-ray spectrum of lead.

Feynman has shown that if one assumes that these x-ray lines are produced by fluorescence in the lead jaws of the source holder, it would be natural to expect the line profile produced by a singlet x-ray line to have a rather complicated but symmetrical shape and the doublets referred to above would therefore appear as exactly mirrored profiles. Because of the small likelihood of complicated multiplets appearing in gamma spectra and the excellent agreement with the $K\beta$ wavelengths of lead, this explanation appears to be the correct one.

The $K\alpha_1$ line of lead appears in the proper place to explain the appearance of the two peaks at 165.567 and 165.136 milliangstroms which previously remained unidentified. These two peaks result, no doubt, from fluorescence excited in the two lead source jaws. Although the $K\alpha_2$ line of lead should also appear in a similar form, it was apparently overlooked while searching past its expected position.